

*Electronic Supplementary information*

**Catalytic hydrothiolation of alkenes and alkynes using bimetallic  
RuRh nanoparticles on carbon nanotubes**

Dhanaji V. Jawale, Frédéric Fossard, Frédéric Miserque, Joël Armel Tchuiteng Kouatchou,  
Valérie Geertsen, Edmond Gravel and Eric Doris

**Table of content**

1. General .....	S2
2. Ru-Rh particle synthesis .....	S2
3. Assembly of Ru-Rh nanoparticles on carbon nanotubes .....	S2
4. Spectroscopic data .....	S2
5. Copies of NMR spectra .....	S6
6. Supplementary Figures .....	S24
7. Supplementary Tables .....	S28

## 1. General

Chemicals and solvents were purchased from commercial suppliers. Flash chromatography was carried out on Kieselgel 60 (230–240 mesh, Merck) and analytical TLC was performed on Merck precoated silica gel (60 F254). Compounds were visualized under UV light and/or by treatment with a solution of phosphomolybdic acid in ethanol followed by heating. NMR spectra were recorded on a Bruker Avance spectrometer at 400 MHz (<sup>1</sup>H), 100 MHz (<sup>13</sup>C), 376 MHz (<sup>19</sup>F) and 61 MHz (<sup>2</sup>H). Chemical shifts are given in ppm relative to the NMR solvent residual peak, coupling constants J are given in Hz. Unless otherwise specified, ultrasonic mixing was achieved using a Branson sonifier 550 equipped with a 3 mm tapered microtip (300 ms/s pulses, Output power 50%). Photo-polymerization experiments are carried out using a 40 W low-pressure mercury UV lamp (Heraeus) emitting at a wavelength of 254 nm. For HRSTEM experiments, a Titan-G2 probe corrected STEM was used to study the Ru/Rh repartition on the carbon nanotubes. The emitted X-rays were collected by the four detectors with a 0.7 steradian collecting angle. The probe was smaller than 2 Å and its current was almost 250 pA. K-Lines were used to distinguish Ru and Rh as illustrated in Figure S1.

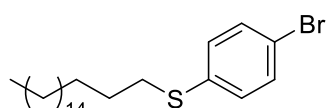
## 2. Ru-Rh particle synthesis

The synthesis of nanoparticles was achieved using a previously reported procedure (*Chem. Mater.*, 2000, **12**, 1622). A solution of RhCl<sub>3</sub>·3H<sub>2</sub>O (39.5 mg, 0.15 mmol) and RuCl<sub>3</sub>·6H<sub>2</sub>O (47.5 mg, 0.15 mmol) in water (5 mL) was mixed with ethylene glycol (100 mL). An aqueous solution of NaOH 0.5 M (5 mL) was added to the stirred mixture and the reaction was heated to 160 °C. After 3 h, a stable transparent brown homogeneous colloid of Ru-Rh NPs was formed.

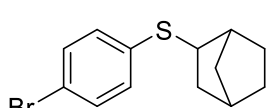
## 3. Assembly of Ru-Rh nanoparticles on carbon nanotubes

The assembly of Ru-Rh nanoparticles at the surface of carbon nanotubes was achieved according to our previously reported procedure (*Angew. Chem. Int. Ed.*, 2011, **50**, 7533).

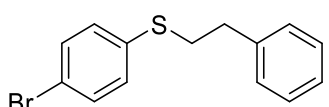
## 4. Spectroscopic data



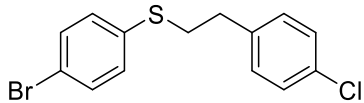
<sup>1</sup>H-NMR (400 MHz, CDCl<sub>3</sub>) δ 0.88 (t, 3H), 1.17–1.45 (m, 30H), 1.59–1.66 (m, 2H), 2.88 (t, 2H), 7.16 (d, 2H, ArH), 7.37 (d, 2H, ArH) ppm. <sup>13</sup>C-NMR (100 MHz, CDCl<sub>3</sub>) δ 14.1, 22.7, 28.8, 29.0, 29.1, 29.4, 29.5, 29.6, 29.6, 29.7, 29.7, 31.9, 33.7, 119.3, 130.3, 131.8, 136.3 ppm.



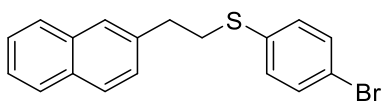
<sup>1</sup>H-NMR (400 MHz, CDCl<sub>3</sub>) δ 1.19–1.24 (m, 3H), 1.37–1.43 (m, 1H), 1.49–1.68 (m, 3H), 1.77–1.83 (m, 1H), 2.24–2.25 (m, 1H), 2.31 (m, 1H), 3.13–3.17 (m, 1H), 7.14–7.18 (m, 2H, ArH), 7.36–7.40 (m, 2H, ArH) ppm. <sup>13</sup>C-NMR (100 MHz, CDCl<sub>3</sub>) δ 28.7, 28.9, 35.6, 36.5, 38.5, 42.2, 119.3, 130.5, 131.8, 137.0 ppm.



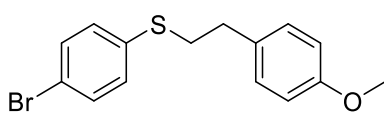
<sup>1</sup>H-NMR (400 MHz, CDCl<sub>3</sub>) δ 2.90–2.94 (t, 2H), 3.13–3.17 (t, 2H), 7.17–7.25 (m, 5H), 7.17–7.25 (m, 5H), 7.29–7.33 (m, 2H, ArH), 7.40–7.42 (m, 2H, ArH) ppm. <sup>13</sup>C-NMR (100 MHz, CDCl<sub>3</sub>) δ 35.3, 35.6, 119.9, 126.7, 128.6, 128.7, 130.8, 132.1, 135.8, 140.0 ppm. NMR data are in agreement with literature: *Green Chem.*, 2018, **20**, 4448.



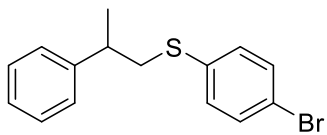
<sup>1</sup>H-NMR (400 MHz, CDCl<sub>3</sub>) δ 2.88–2.92 (t, 2H), 3.12–3.16 (t, 2H), 7.11–7.15 (m, 2H, ArH), 7.20–7.24 (m, 2H, ArH), 7.27–7.31 (m, 2H, ArH), 7.42–7.45 (m, 2H, ArH) ppm. <sup>13</sup>C-NMR (100 MHz, CDCl<sub>3</sub>) δ 34.8, 35.2, 120.0, 128.7, 129.9, 130.9, 132.0, 132.4, 135.3, 138.3 ppm.



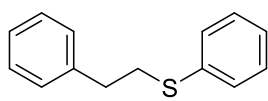
<sup>1</sup>H-NMR (400 MHz, CDCl<sub>3</sub>) δ 3.09–3.13 (t, 2H), 3.24–3.28 (t, 2H), 7.24–7.27 (m, 2H, ArH), 7.33–7.35 (m, 1H, ArH), 7.42–7.51 (m, 4H, ArH), 7.65 (s, 1H, ArH), 7.80–7.85 (m, 3H, ArH) ppm. <sup>13</sup>C-NMR (100 MHz, CDCl<sub>3</sub>) δ 35.1, 35.7, 119.9, 125.6, 126.2, 126.9, 126.9, 127.5, 127.7, 128.2, 130.8, 132.0, 132.3, 133.5, 135.6, 137.3 ppm.



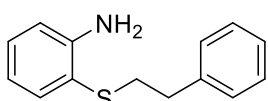
<sup>1</sup>H-NMR (400 MHz, CDCl<sub>3</sub>) δ 2.86–2.90 (t, 2H), 3.12–3.16 (t, 2H), 3.82 (s, 3H), 6.85–6.88 (m, 2H, ArH), 7.11–7.15 (m, 2H, ArH), 7.20–7.28 (m, 2H, ArH), 7.41–7.44 (m, 2H, ArH) ppm. <sup>13</sup>C-NMR (100 MHz, CDCl<sub>3</sub>) δ 34.6, 35.5, 114.0, 119.7, 129.5, 130.7, 131.9, 135.8, 158.3 ppm.



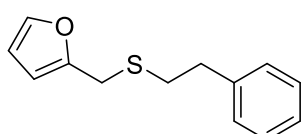
<sup>1</sup>H-NMR (400 MHz, CDCl<sub>3</sub>) δ 1.41 (d, 3H), 3.09–3.13 (t, 2H), 2.94–3.10 (m, 2H), 3.19–3.23 (m, 1H), 7.16–7.28 (m, 5H, ArH), 7.32–7.37 (m, 2H, ArH), 7.38–7.42 (m, 2H, ArH) ppm. <sup>13</sup>C-NMR (100 MHz, CDCl<sub>3</sub>) δ 21.0, 39.4, 42.1, 119.6, 126.7, 126.9, 128.6, 130.6, 131.9, 136.1, 146.2 ppm. NMR data are in agreement with literature: *J. Org. Chem.*, 1982, **47**, 2261.



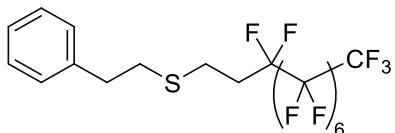
<sup>1</sup>H-NMR (400 MHz, CDCl<sub>3</sub>) δ 2.94–2.98 (t, 2H), 3.18–3.22 (t, 1H), 7.20–7.28 (m, 4H, ArH), 7.31–7.34 (m, 4H, ArH), 7.38–7.40 (m, 2H, ArH) ppm. <sup>13</sup>C-NMR (100 MHz, CDCl<sub>3</sub>) δ 35.1, 35.7, 126.0, 126.5, 128.5, 129.0, 129.2, 136.4, 140.2 ppm.



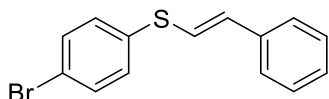
<sup>1</sup>H-NMR (400 MHz, CDCl<sub>3</sub>) δ 2.76–2.79 (t, 2H), 2.90–2.94 (t, 1H), 4.22 (br s, 2H), 6.60–6.66 (m, 2H, ArH), 7.03–7.14 (m, 4H, ArH), 7.17–7.22 (m, 2H, ArH), 7.31–7.33 (m, 2H, ArH), 7.32–7.33 (m, 1H, ArH) ppm. <sup>13</sup>C-NMR (100 MHz, CDCl<sub>3</sub>) δ 36.0, 36.1, 114.9, 117.7, 118.5, 126.3, 128.5, 128.6, 129.7, 135.8, 140.4, 148.3 ppm. NMR data are in agreement with literature: *Chem. Eur. J.*, 2009, **15**, 3666.



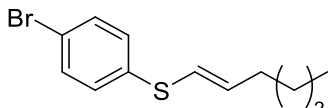
<sup>1</sup>H-NMR (400 MHz, CDCl<sub>3</sub>) δ 2.68–2.72 (t, 2H), 2.78–2.82 (t, 1H), 3.68 (s, 2H), 6.13–6.14 (m, 1H), 6.26–6.28 (m, 1H), 7.13–7.19 (m, 3H, ArH), 7.21–7.27 (m, 2H, ArH), 7.32–7.33 (m, 1H, ArH) ppm. <sup>13</sup>C-NMR (100 MHz, CDCl<sub>3</sub>) δ 28.4, 33.1, 36.0, 107.5, 110.4, 126.3, 128.4, 128.5, 140.4, 142.1, 151.6 ppm. NMR data are in agreement with literature: *Adv. Synth. Catal.*, 2017, **359**, 323.



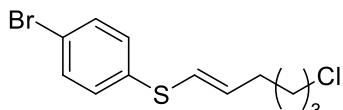
<sup>1</sup>H-NMR (400 MHz, CDCl<sub>3</sub>) δ 2.31–2.45 (m, 2H), 2.74–2.78 (m, 2H), 2.83–2.88 (m, 2H), 2.92–2.96 (m, 2H), 7.24–7.29 (m, 3H, ArH), 7.33–7.37 (m, 2H, ArH) ppm. <sup>13</sup>C-NMR (100 MHz, CDCl<sub>3</sub>) δ 22.8, 22.8, 22.9, 31.9, 32.1, 32.3, 33.8, 36.1, 126.6, 128.5, 128.6, 140.0 ppm. <sup>19</sup>F-NMR (376 MHz, CDCl<sub>3</sub>) δ -126.2, -123.4, -122.8, -122.8, -114.4, -80.8 ppm. H-statements for heptadecafluoro-1-decanethiol: H302/H332/H318/H351/H360D/H362/H372.



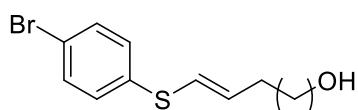
<sup>1</sup>H-NMR (400 MHz, CDCl<sub>3</sub>) δ 6.77–6.87 (m, 2H), 7.27 (m, 3H, ArH), 7.30 (m, 4H, ArH), 7.47 (m, 2H, ArH) ppm. <sup>13</sup>C-NMR (100 MHz, CDCl<sub>3</sub>) δ 120.9, 122.3, 126.1, 127.9, 128.8, 131.1, 132.2, 133.1, 134.6, 136.3 ppm. NMR data are in agreement with literature: *Angew. Chem. Int. Ed.* 2020, **59**, 15512.



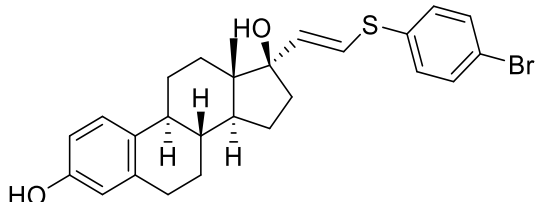
<sup>1</sup>H-NMR (400 MHz, CDCl<sub>3</sub>) δ 0.93 (m, 3H), 1.36–1.54 (m, 4H), 2.16–2.29 (m, 2H), 5.85 (d, minor), 5.85 (d, major), 6.07 (m, major), 6.12 (m, major), 7.14–7.20 (m, 2H, ArH), 7.38–7.44 (m, 2H, ArH) ppm. <sup>13</sup>C-NMR (100 MHz, CDCl<sub>3</sub>) δ 13.9, 22.2, 28.9, 31.1, 32.8, 119.9, 121.7, 129.8, 131.9, 134.9, 136.1, 139.0 ppm. NMR data are in agreement with literature: *Org. Lett.*, 2004, **6**, 5005.



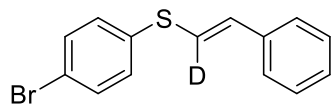
<sup>1</sup>H-NMR (400 MHz, CDCl<sub>3</sub>) δ 1.57–1.64 (m, 2H), 1.78–1.86 (m, 2H), 2.18–2.31 (m, 2H), 3.54–3.58 (m, 2H), 5.81–5.87 (m, major), 5.94–6.04 (m, major), 6.09–6.18 (m, major), 7.15–7.20 (m, 2H, ArH), 7.40–7.43 (m, 2H, ArH) ppm. <sup>13</sup>C-NMR (100 MHz, CDCl<sub>3</sub>) δ 26.2, 28.3, 31.9, 44.8, 121.0, 122.8, 130.0, 130.2, 132.0, 133.5, 137.2 ppm.



<sup>1</sup>H-NMR (400 MHz, CDCl<sub>3</sub>) δ 1.30 (m, 12H), 1.41–1.42 (m, 2H), 1.50–1.60 (m, 2H), 2.14–2.26 (m, 2H), 3.62–3.66 (m, 2H), 5.84–5.90 (m, major), 6.00–6.13 (m, major), 7.14–7.19 (m, 2H, ArH), 7.39–7.41 (m, 2H, ArH) ppm. <sup>13</sup>C-NMR (100 MHz, CDCl<sub>3</sub>) δ 25.7, 28.9, 29.1, 29.4, 29.5, 32.8, 33.1, 63.0, 119.8, 129.7, 130.0, 131.9, 135.0, 136.1, 139.1 ppm.



<sup>1</sup>H-NMR (400 MHz, CDCl<sub>3</sub>) δ 0.68 (s, 3H), 1.38–1.46 (m, 1H), 1.58–2.31 (m, 6H), 2.79–2.84 (m, 2H), 4.56 (s, 1H), 4.91–4.94 (d, 1H), 4.99–5.02 (d, 1H), 6.56 (d, 1H, ArH), 6.64 (m, 1H, ArH), 7.14–7.16 (d, 1H, ArH), 7.33–7.36 (m, 2H, ArH), 7.40–7.43 (m, 2H, ArH) ppm. <sup>13</sup>C-NMR (100 MHz, CDCl<sub>3</sub>) δ 14.2, 18.6, 21.0, 23.8, 26.5, 26.5, 27.5, 29.6, 35.7, 38.5, 44.0, 44.7, 53.1, 54.8, 60.4, 112.7, 115.2, 122.5, 122.6, 126.5, 131.8, 131.9, 132.6, 132.7, 132.8, 135.2, 135.6, 138.2, 153.3, 156.4 ppm. H-statements for 17α-ethynylestradiol: H302/H350.

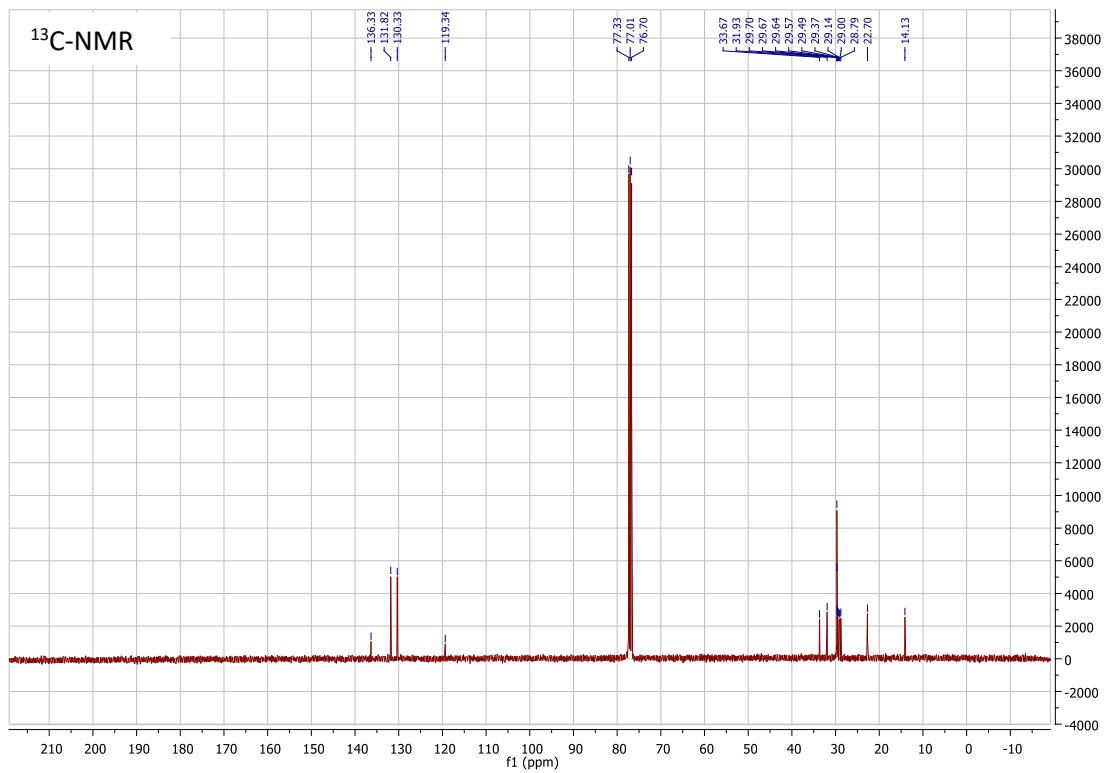
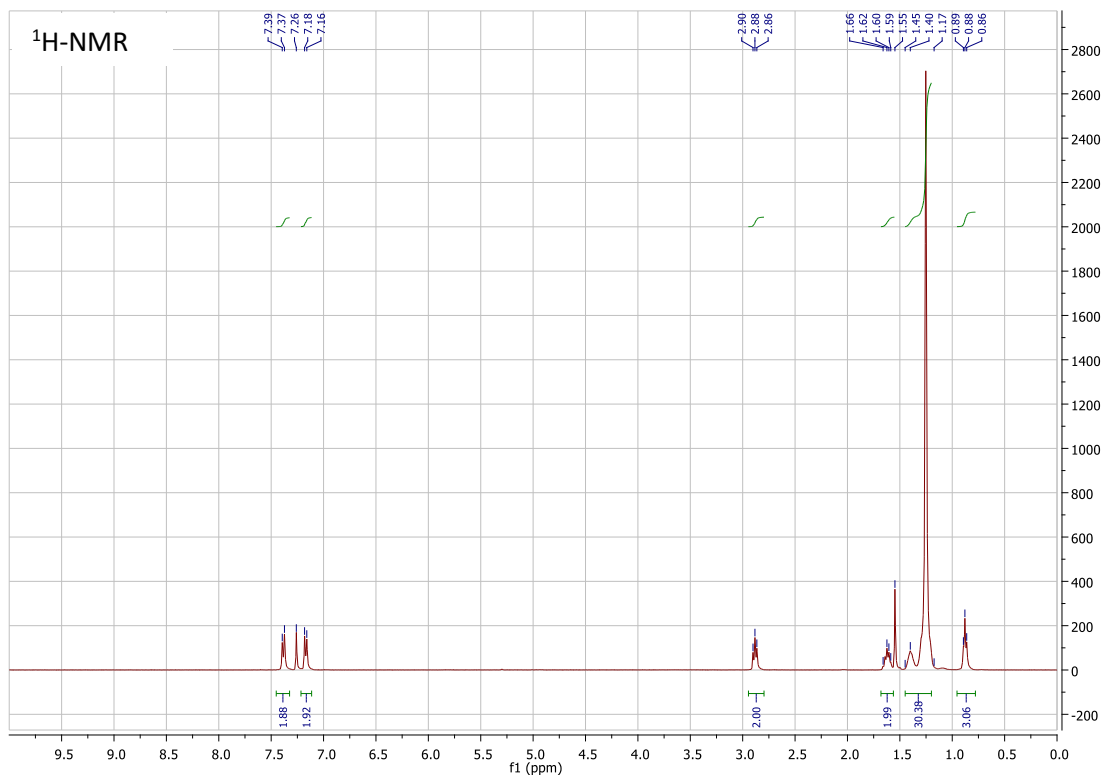
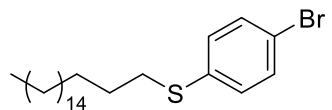


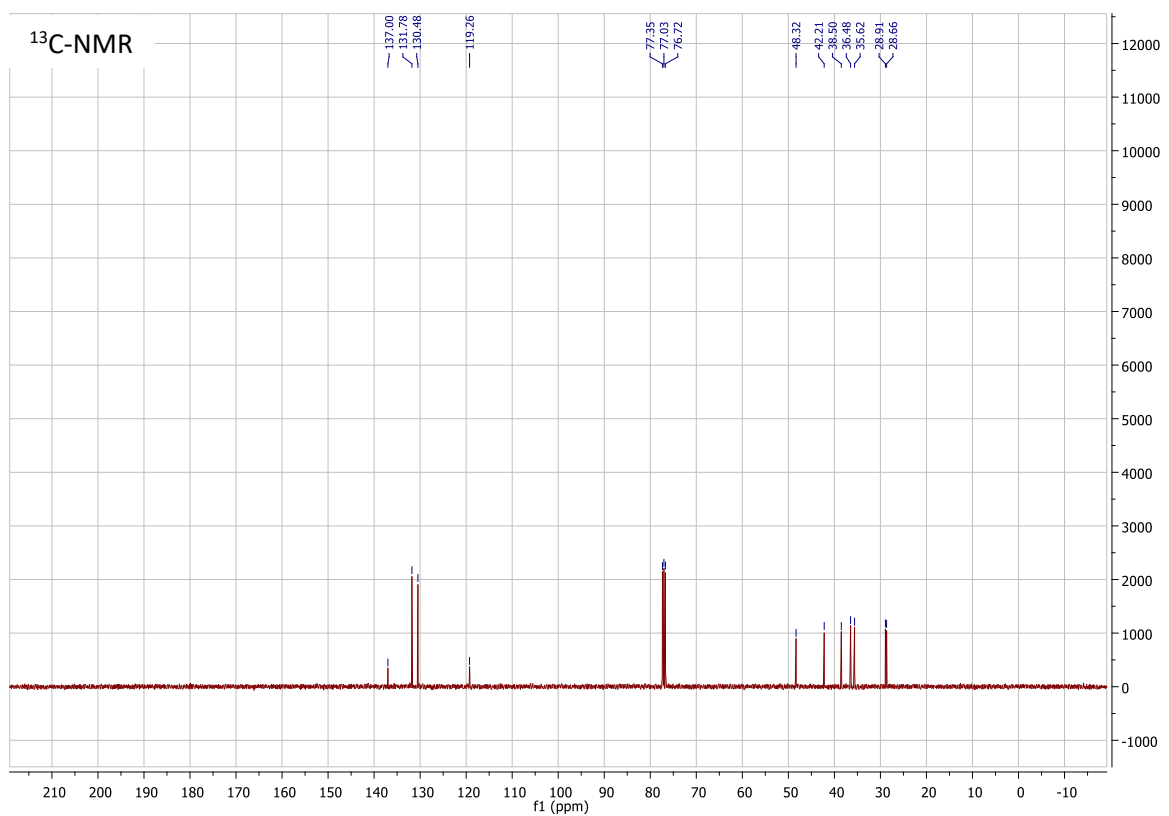
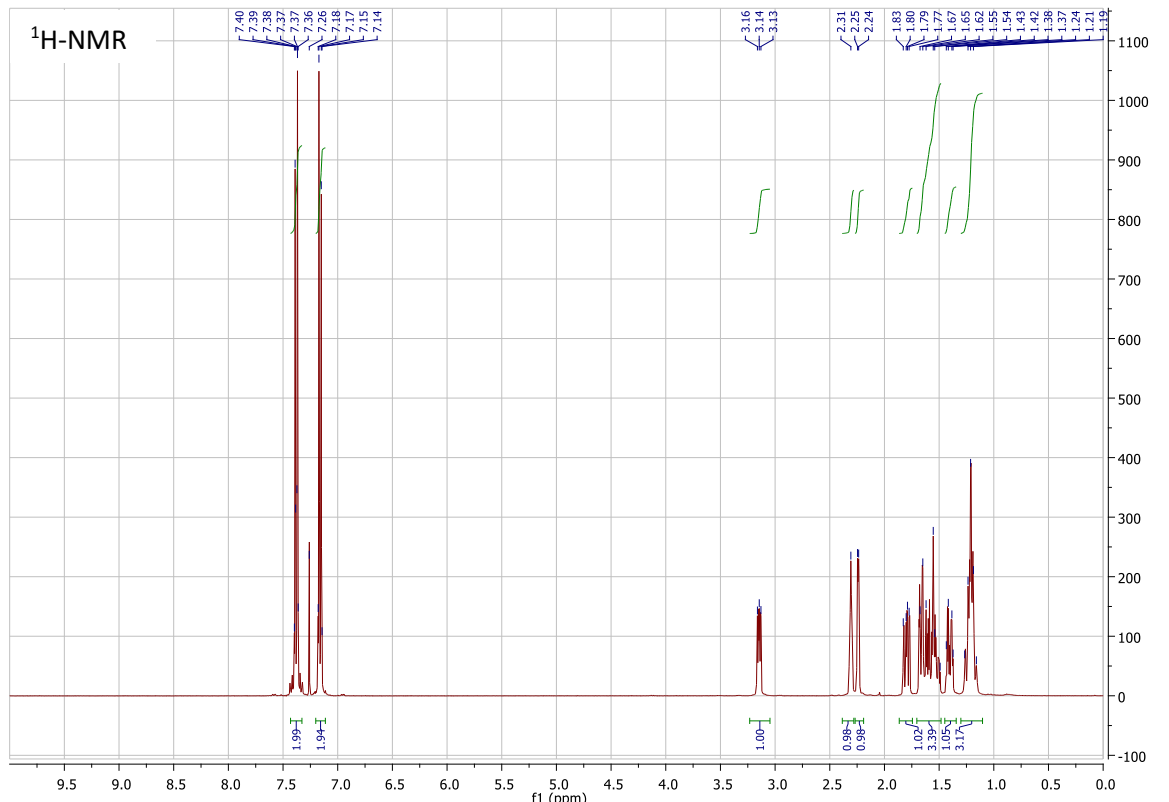
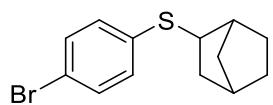
$^1\text{H-NMR}$  (400 MHz,  $\text{CDCl}_3$ )  $\delta$  6.78 (s, 1H), 7.28 (m, 3H, ArH), 7.35 (m, 4H, ArH), 7.47 (m, 2H, ArH) ppm.  $^2\text{H}$ -NMR (61 MHz,  $\text{CHCl}_3$ )  $\delta$  7.00 ppm.  $^{13}\text{C-NMR}$  (100 MHz,  $\text{CDCl}_3$ )  $\delta$  120.9, 122.0 (t), 126.1, 127.9, 128.8, 131.1, 132.2, 132.9, 134.6, 136.3 ppm.

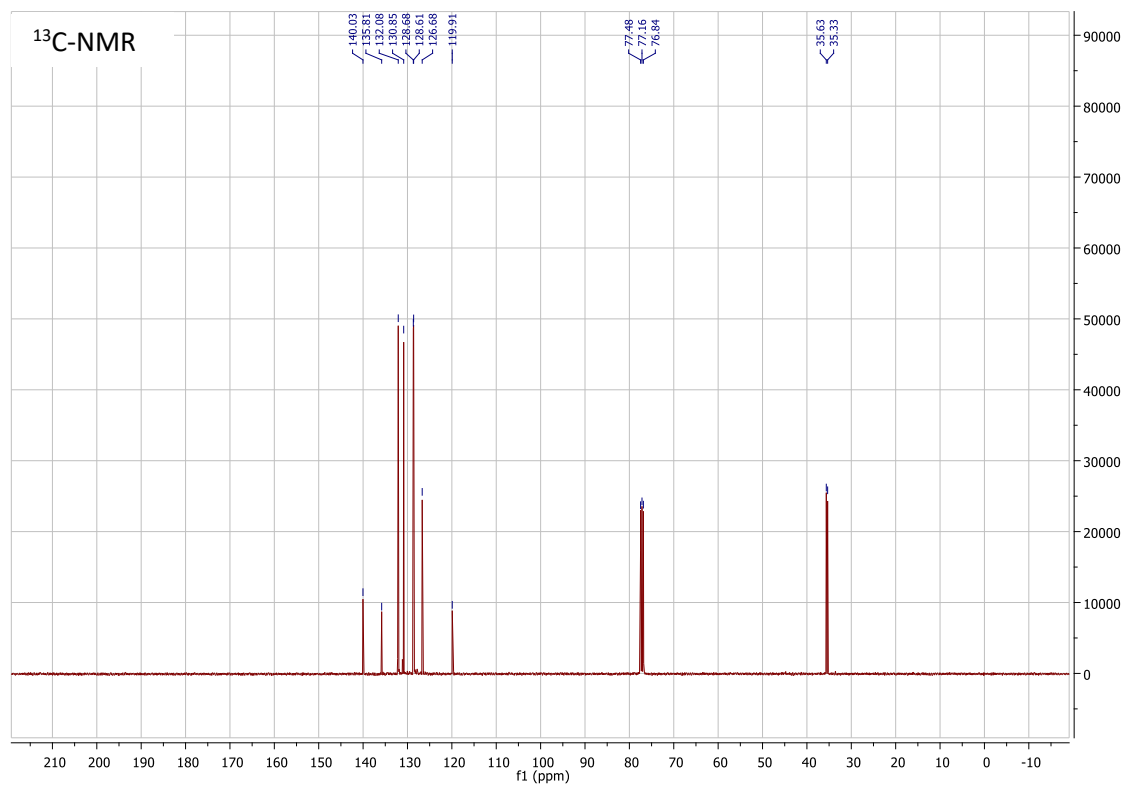
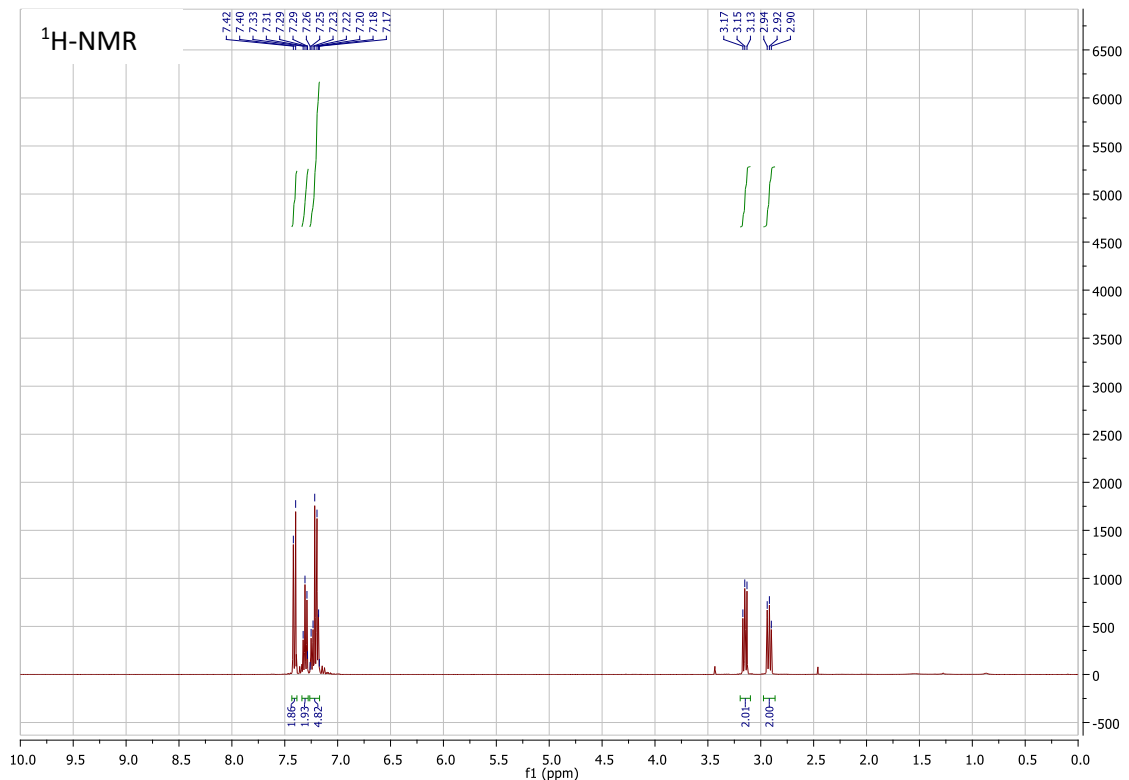
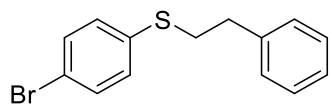


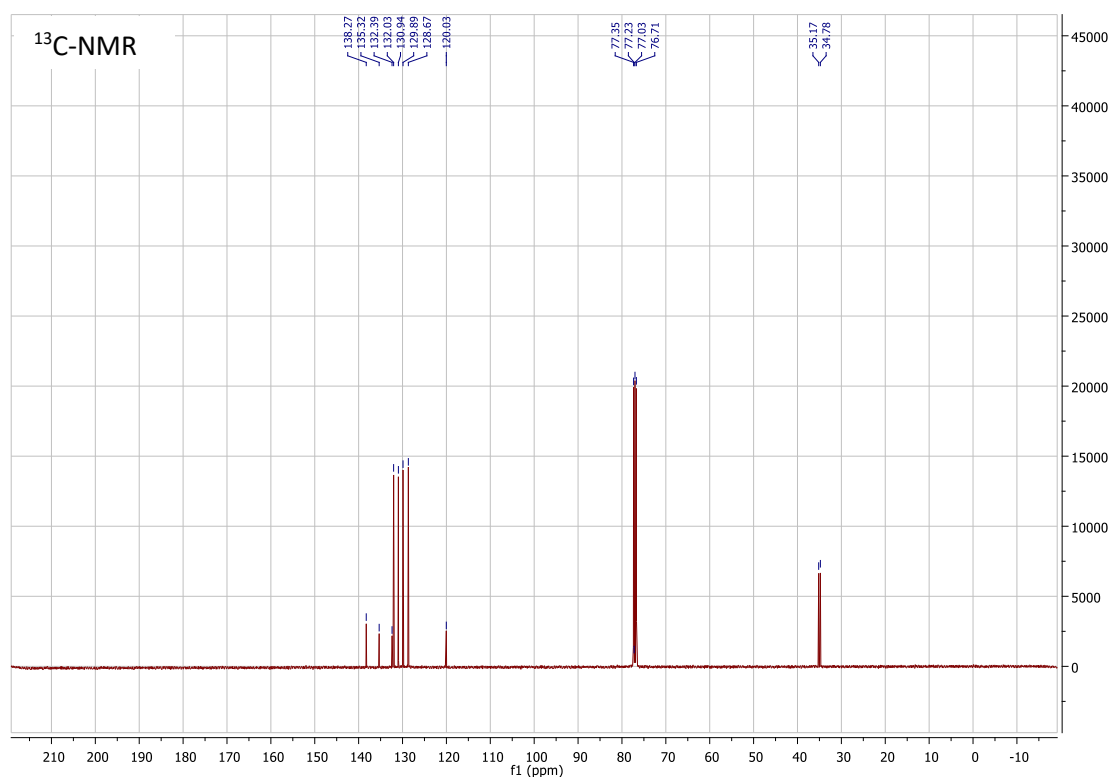
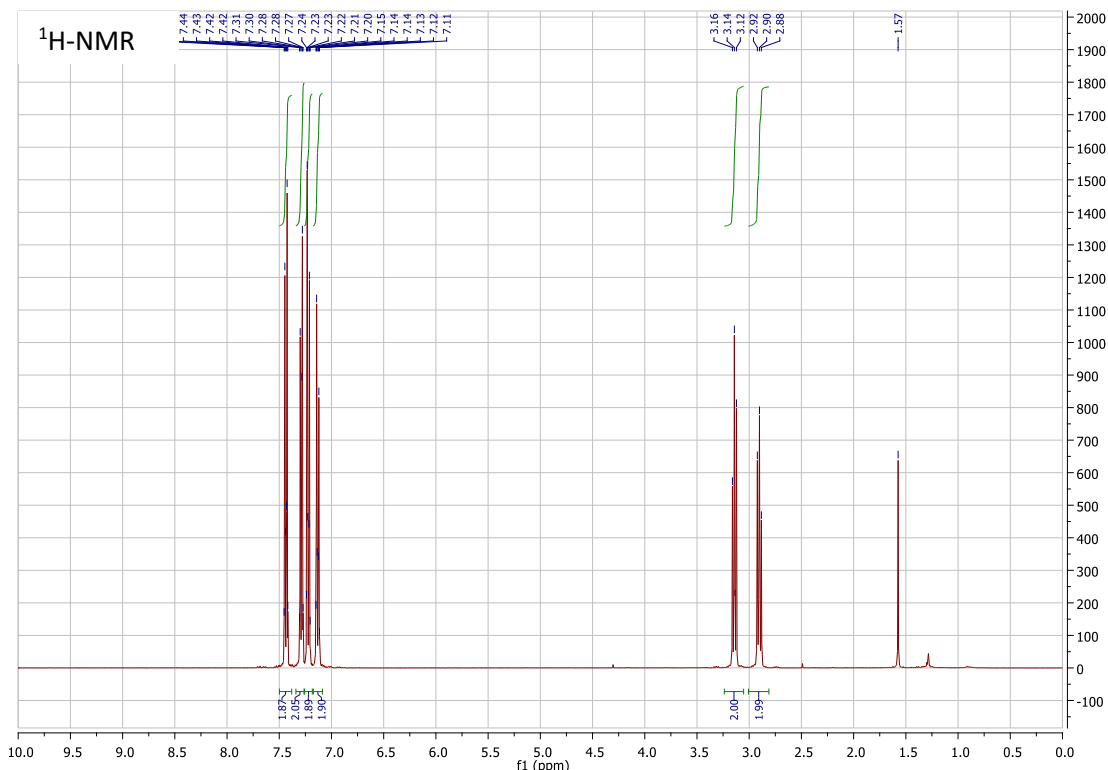
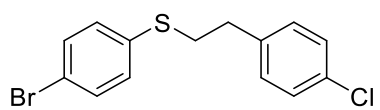
$^1\text{H-NMR}$  (400 MHz,  $\text{CDCl}_3$ )  $\delta$  6.71 (m, 1H), 7.21 (m, 3H, ArH), 7.29 (m, 4H, ArH), 7.39 (m, 2H, ArH) ppm.  $^2\text{H-NMR}$  (61 MHz,  $\text{CHCl}_3$ )  $\delta$  6.97 ppm.  $^{13}\text{C-NMR}$  (100 MHz,  $\text{CDCl}_3$ )  $\delta$  120.9, 122.1, 126.1, 127.9, 128.8, 131.1, 132.0 (t), 133.0, 133.0, 134.6, 136.2 ppm.

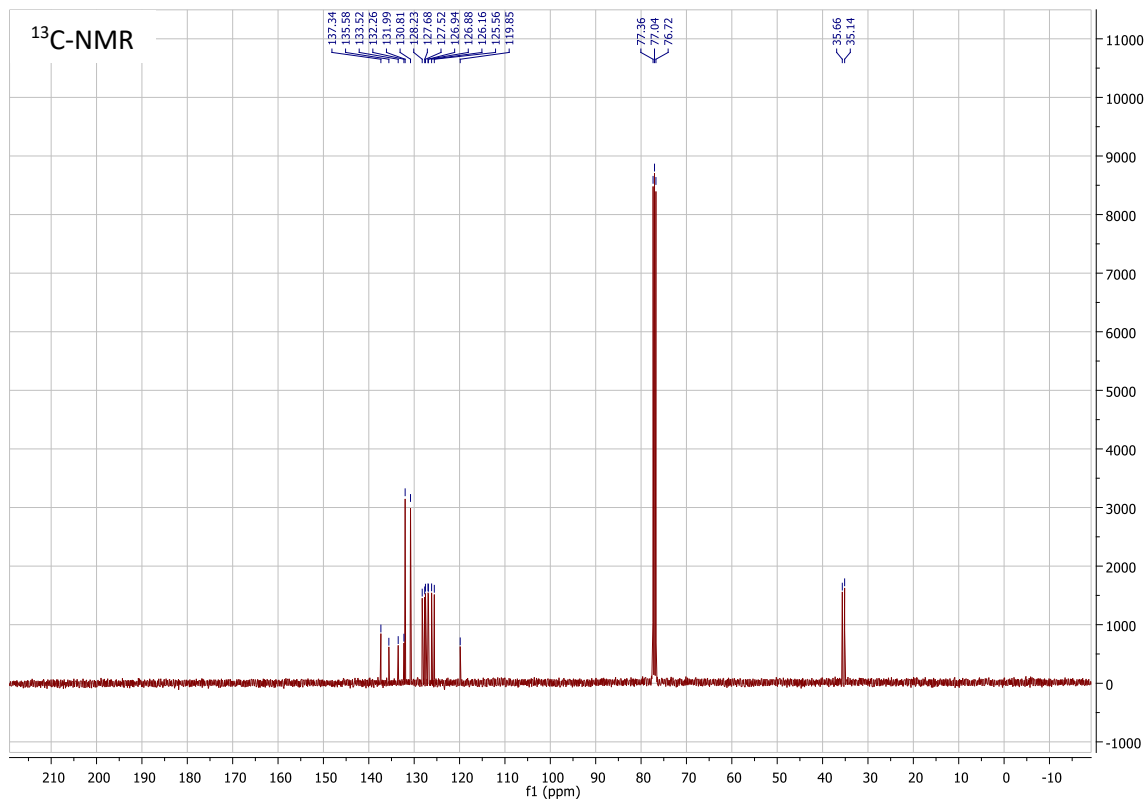
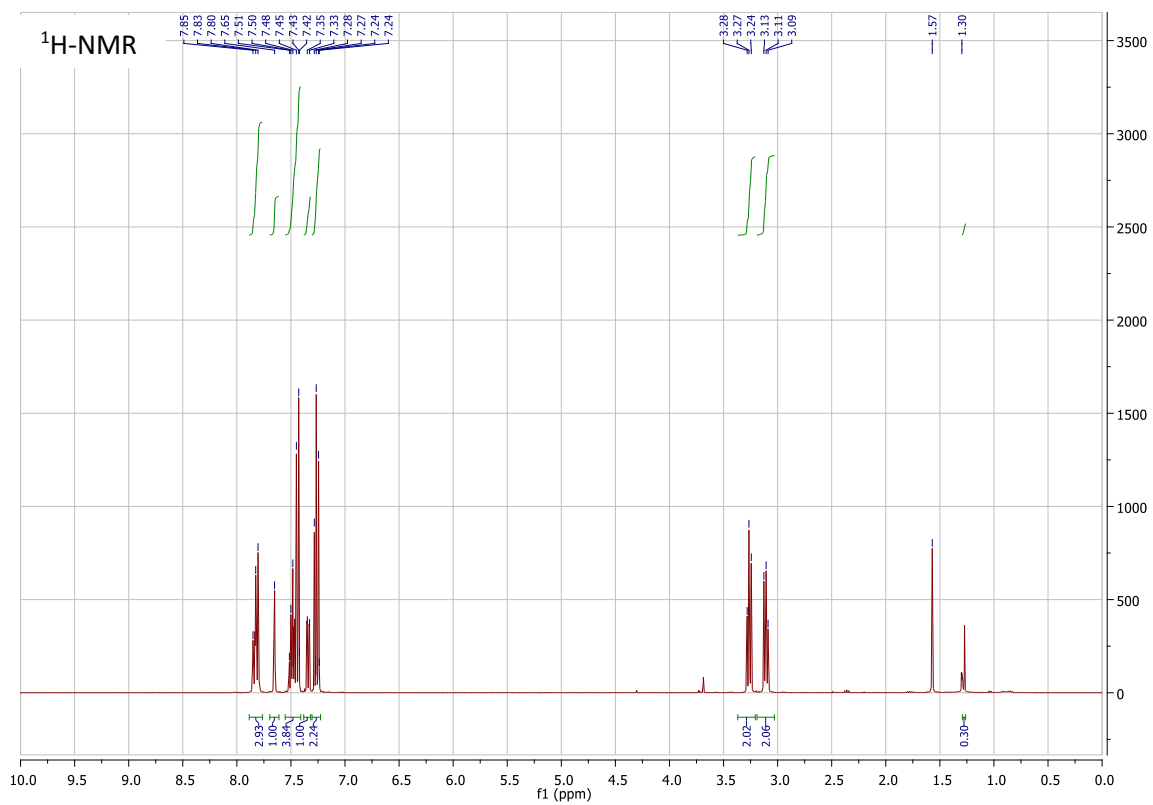
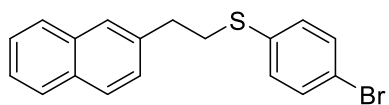
## 5. Copies of NMR spectra

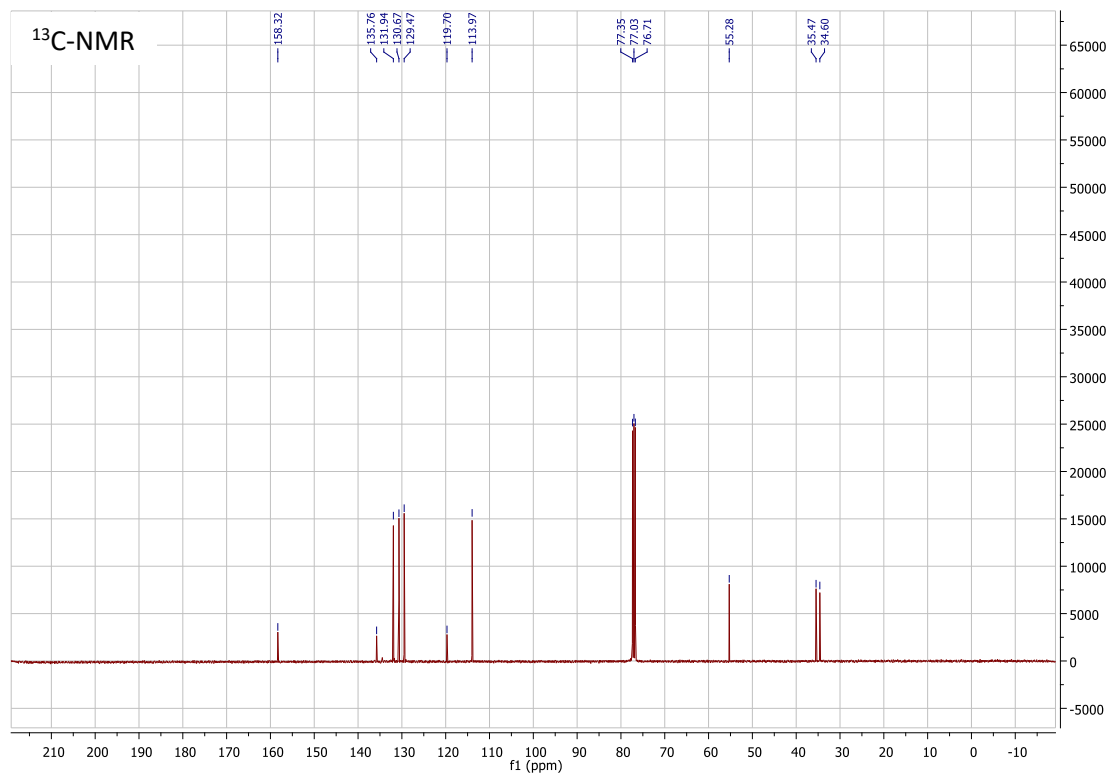
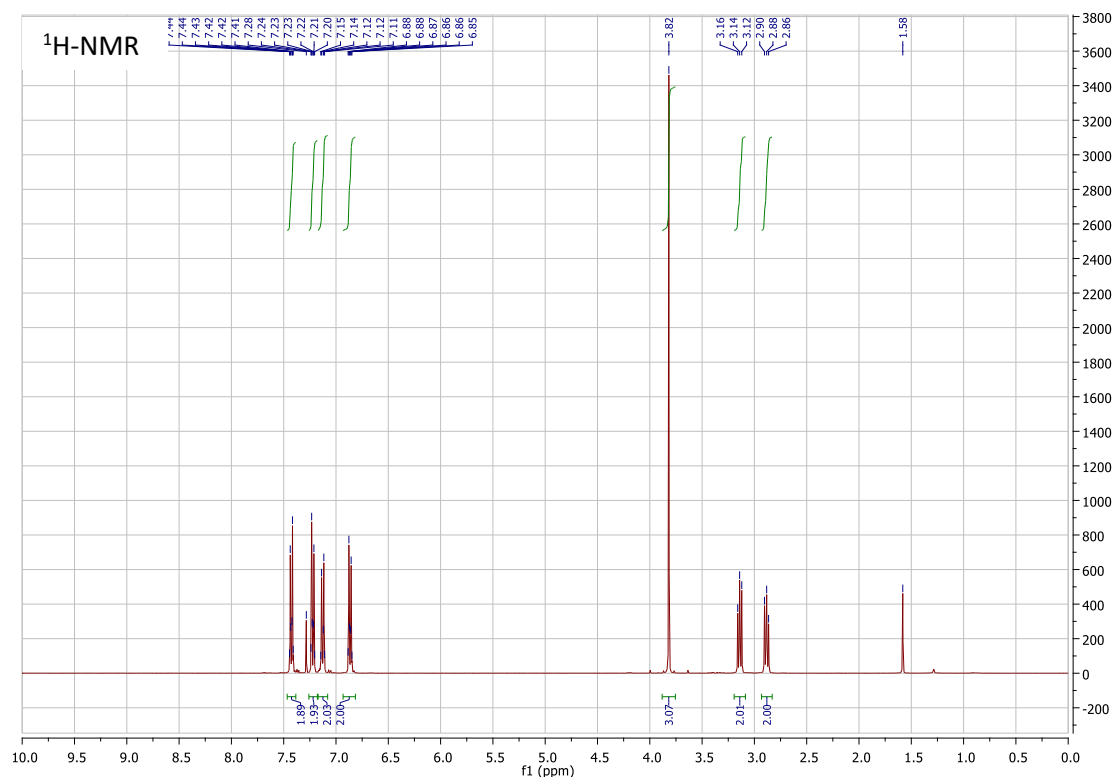
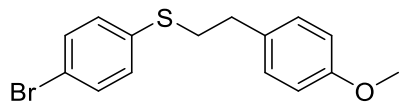


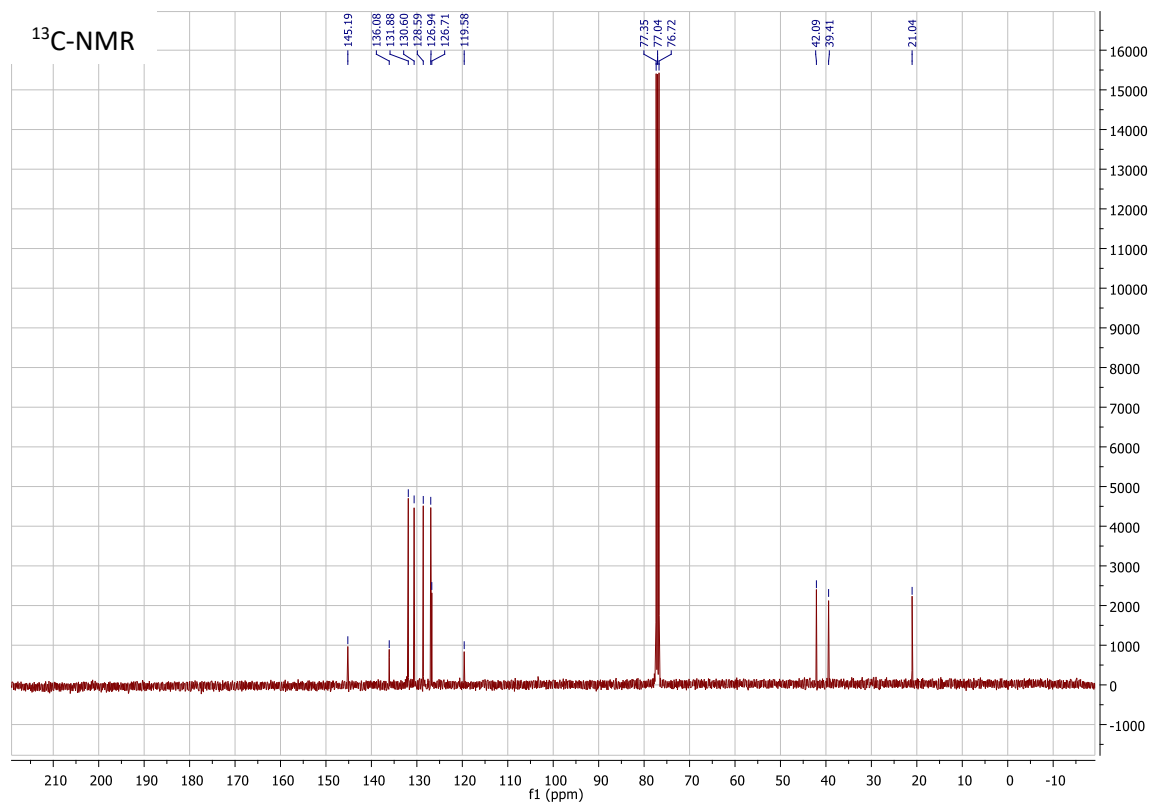
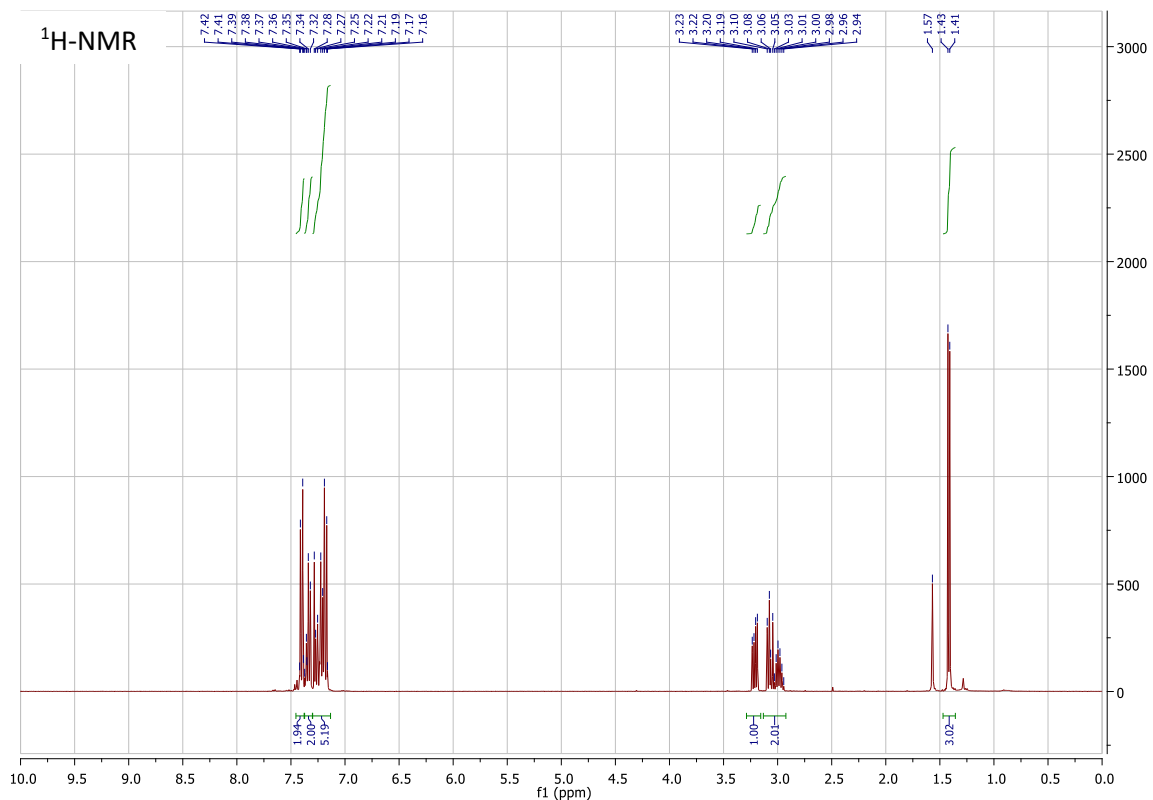
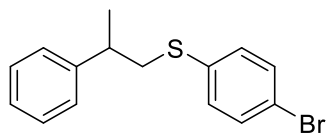


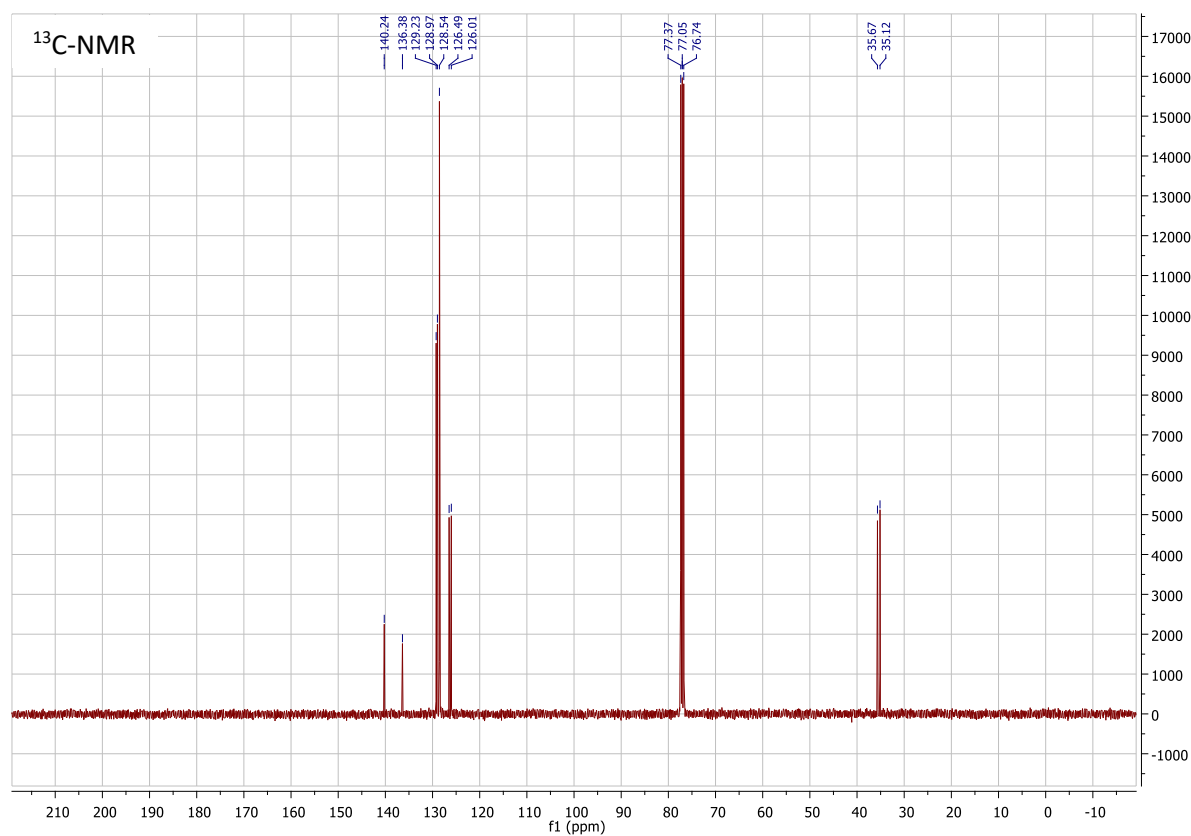
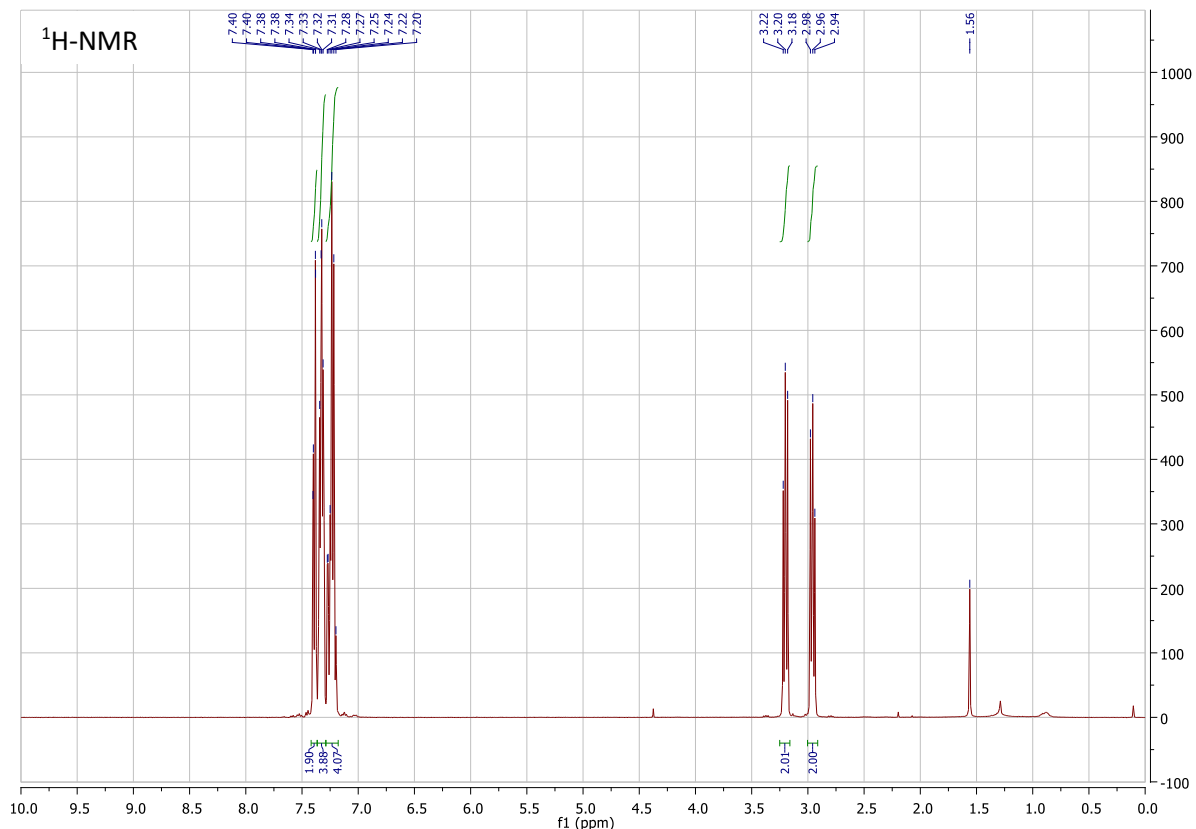
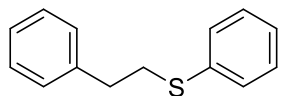


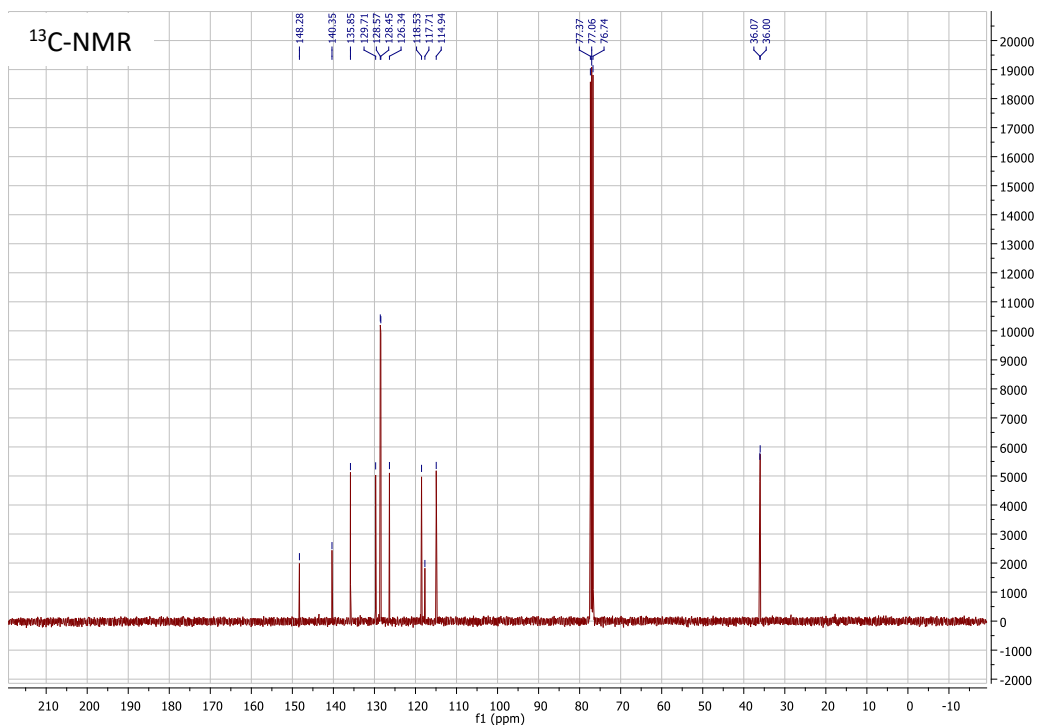
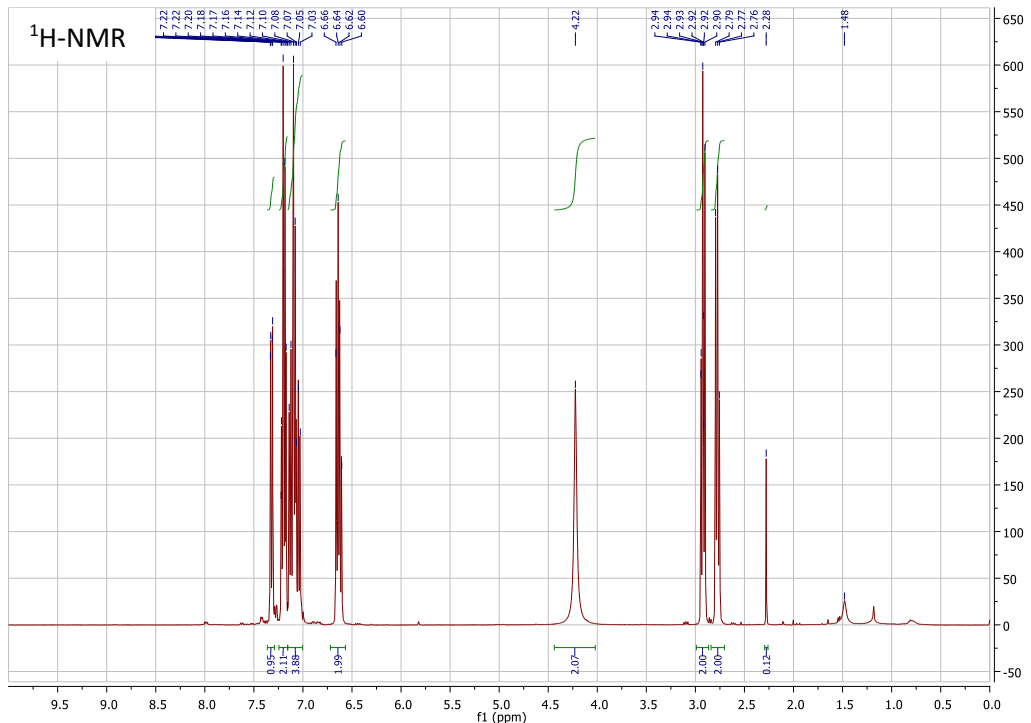
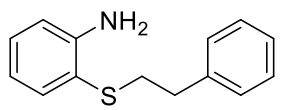


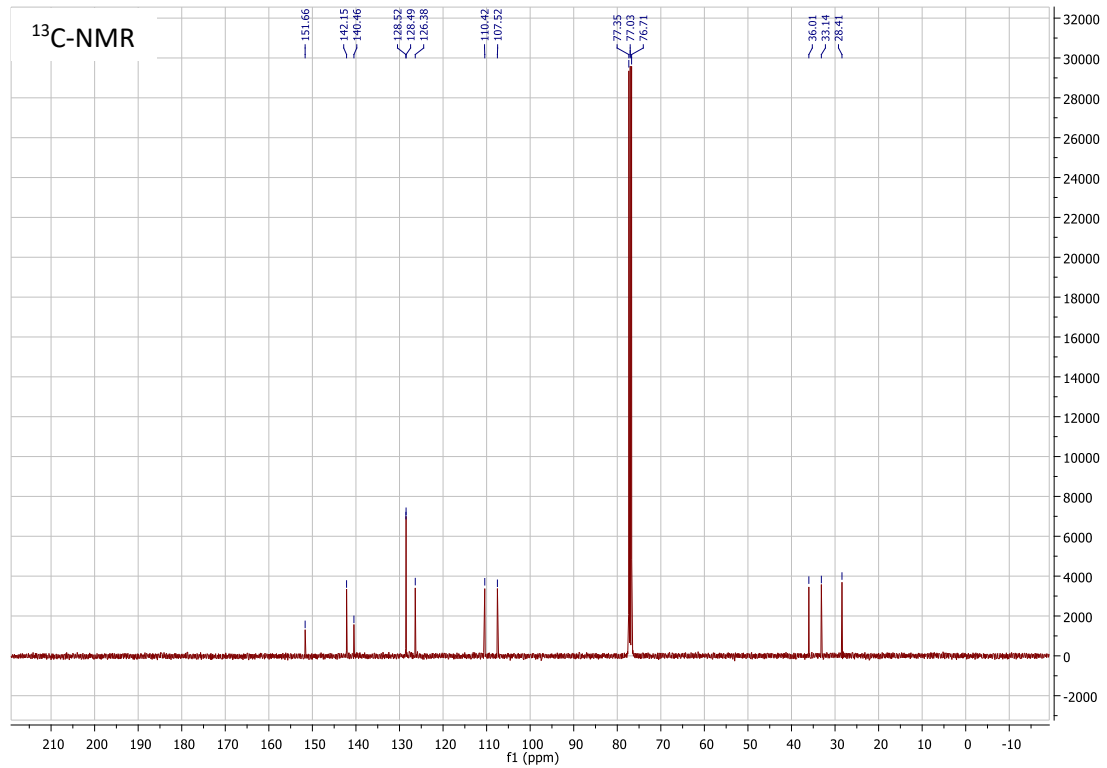
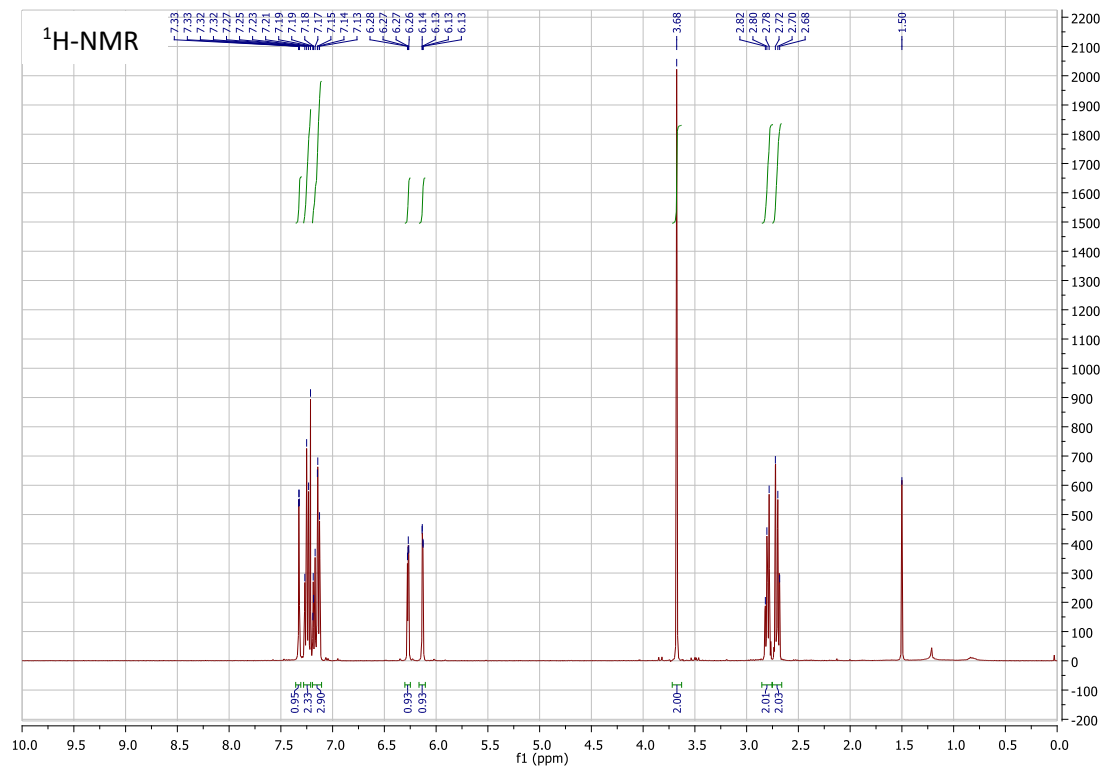
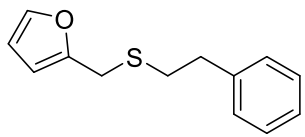


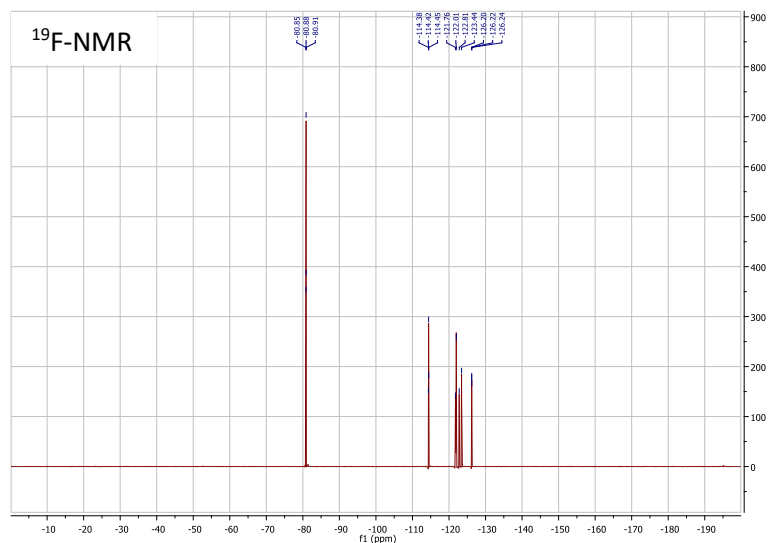
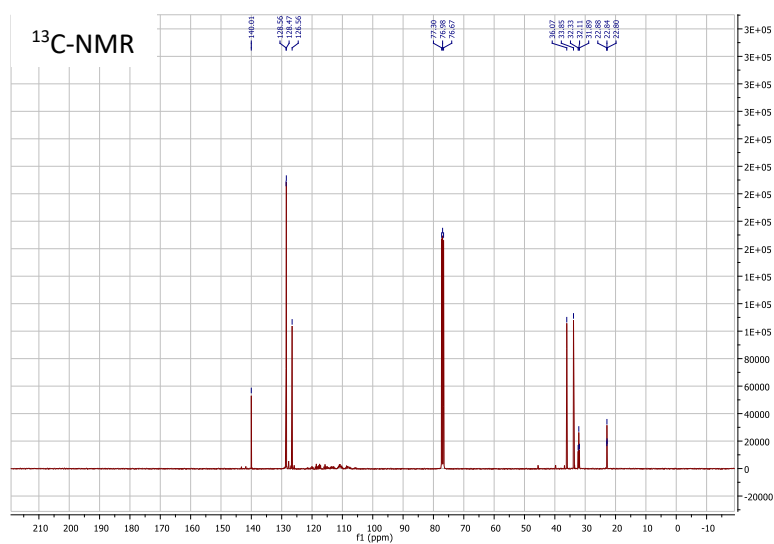
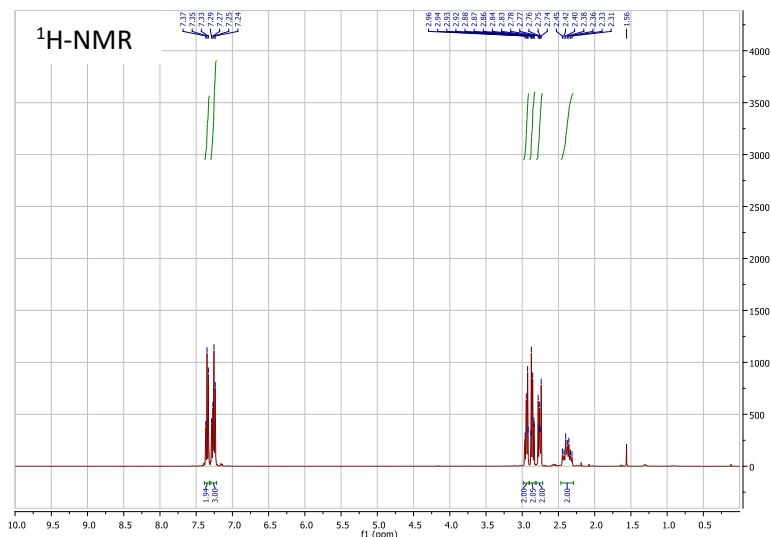
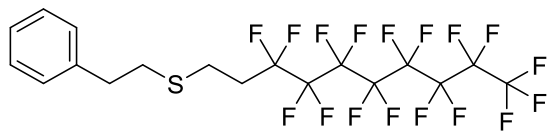


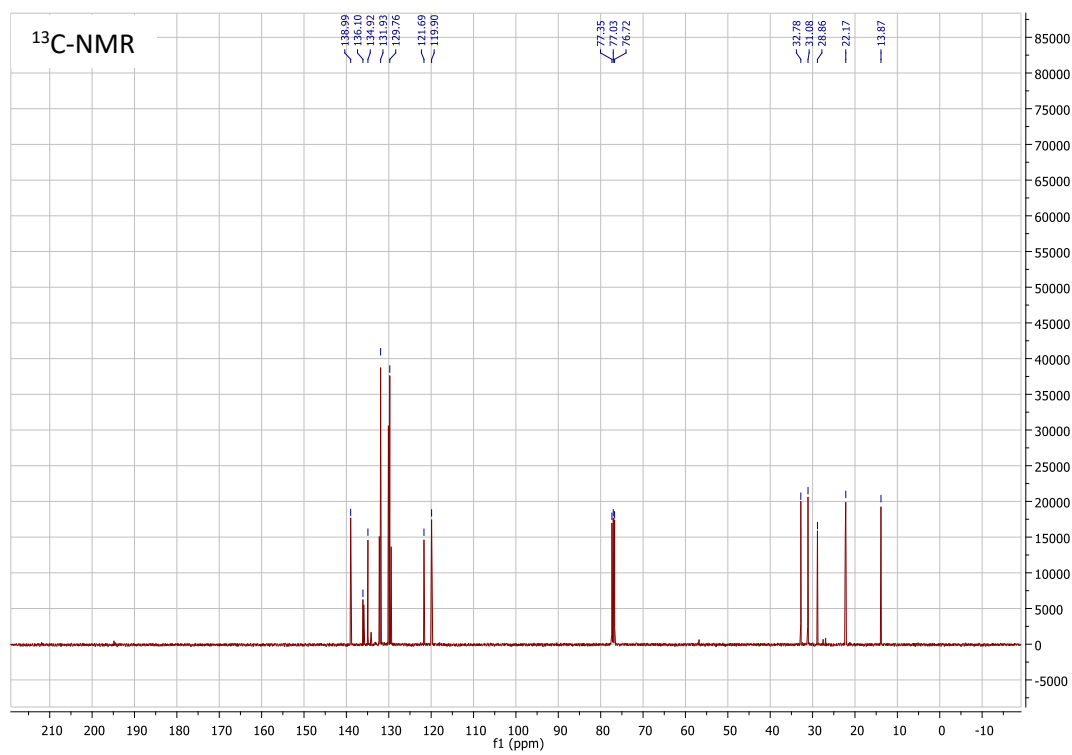
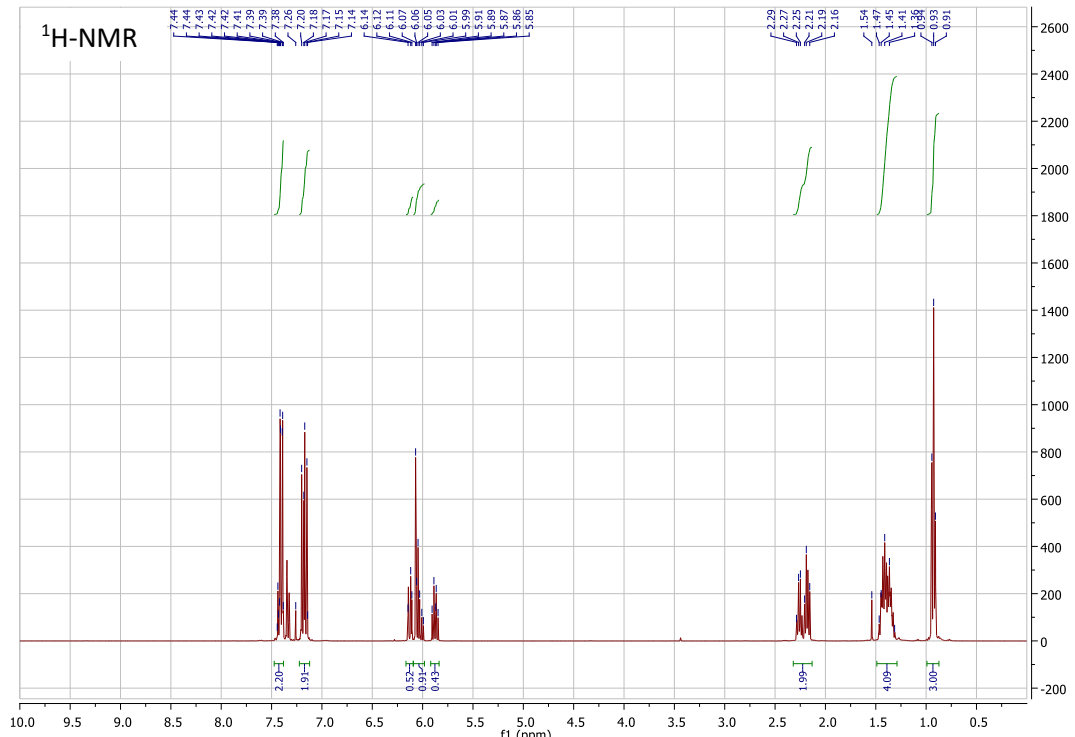
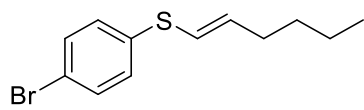


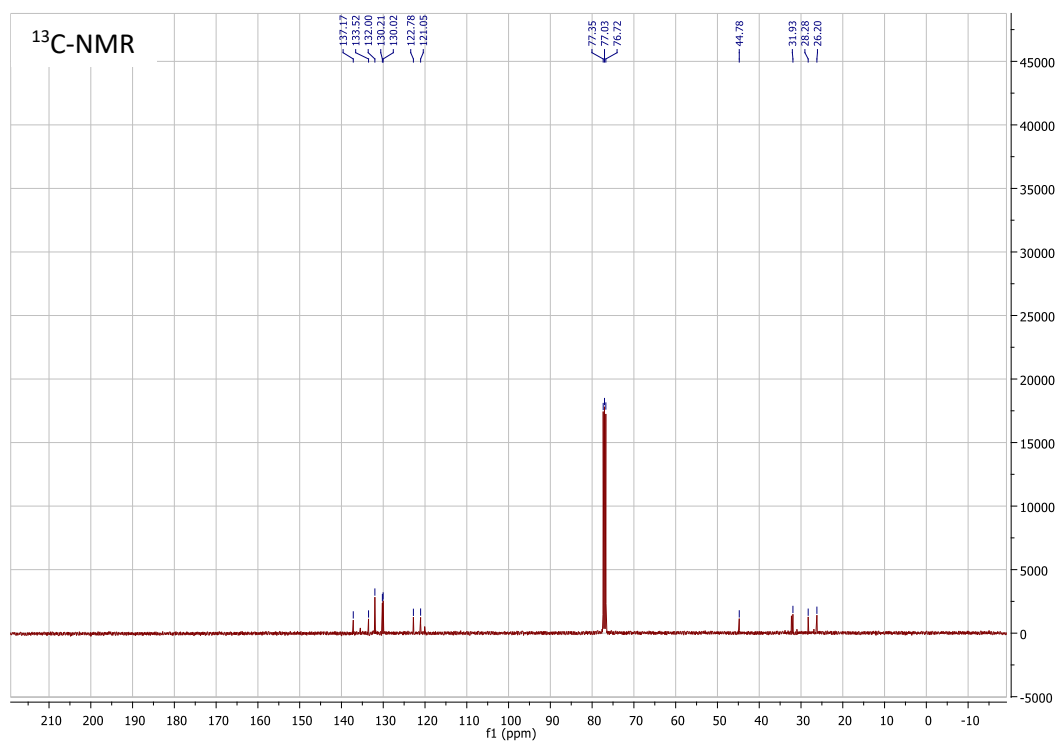
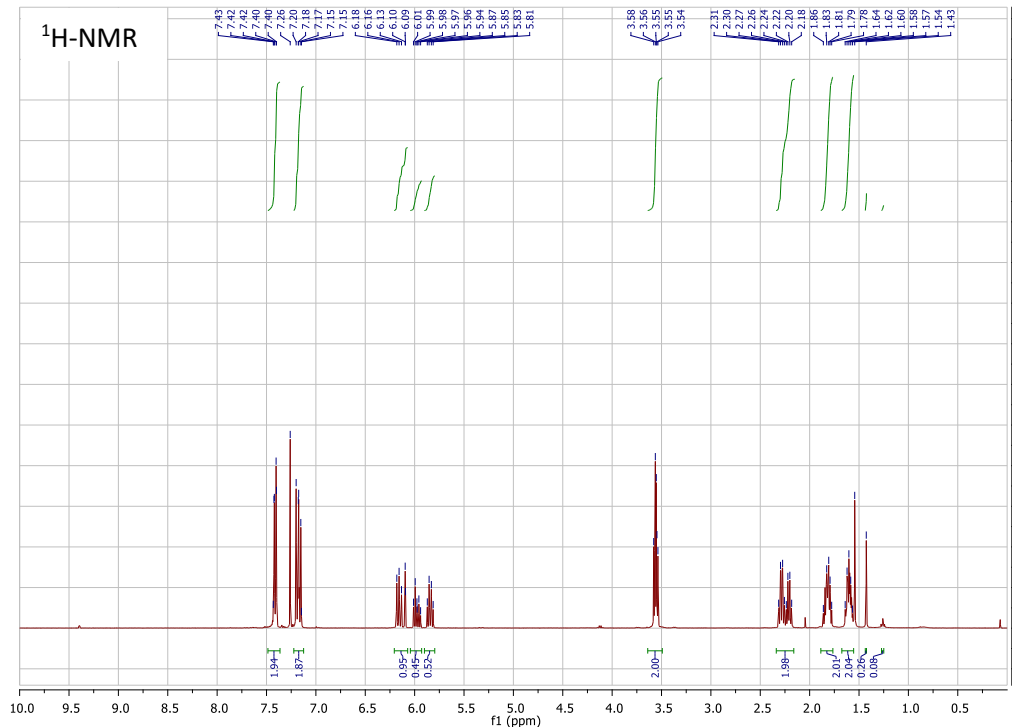
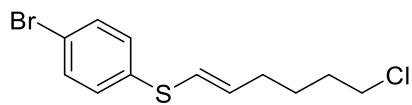


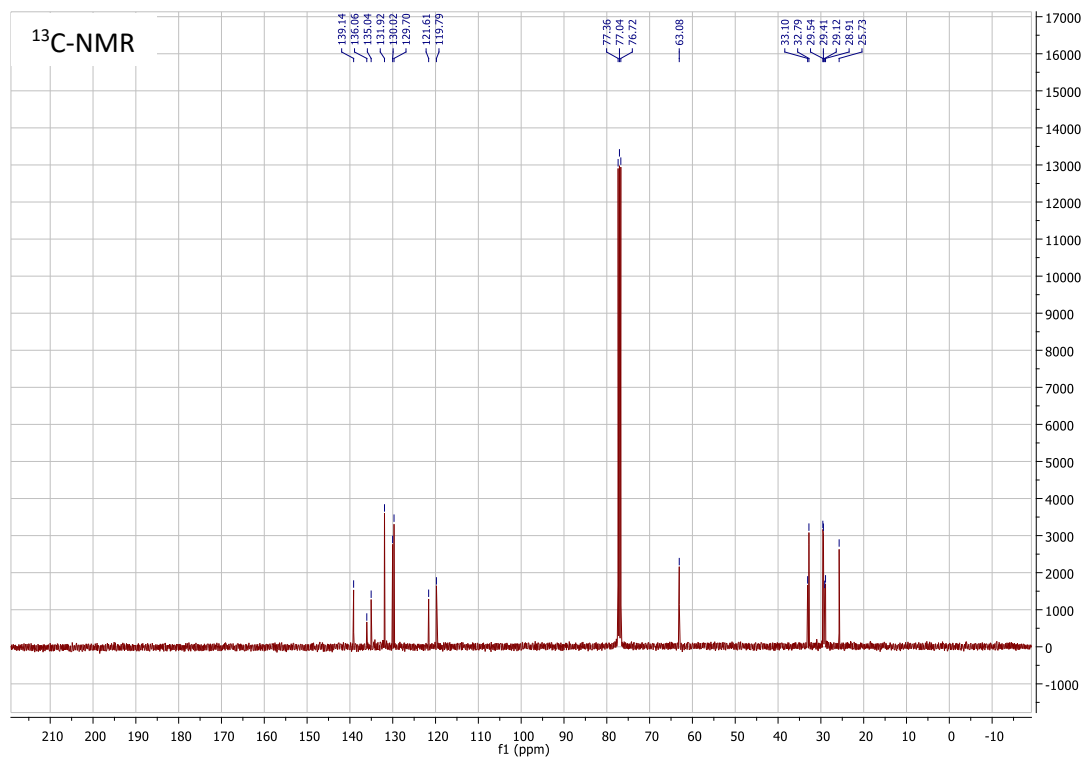
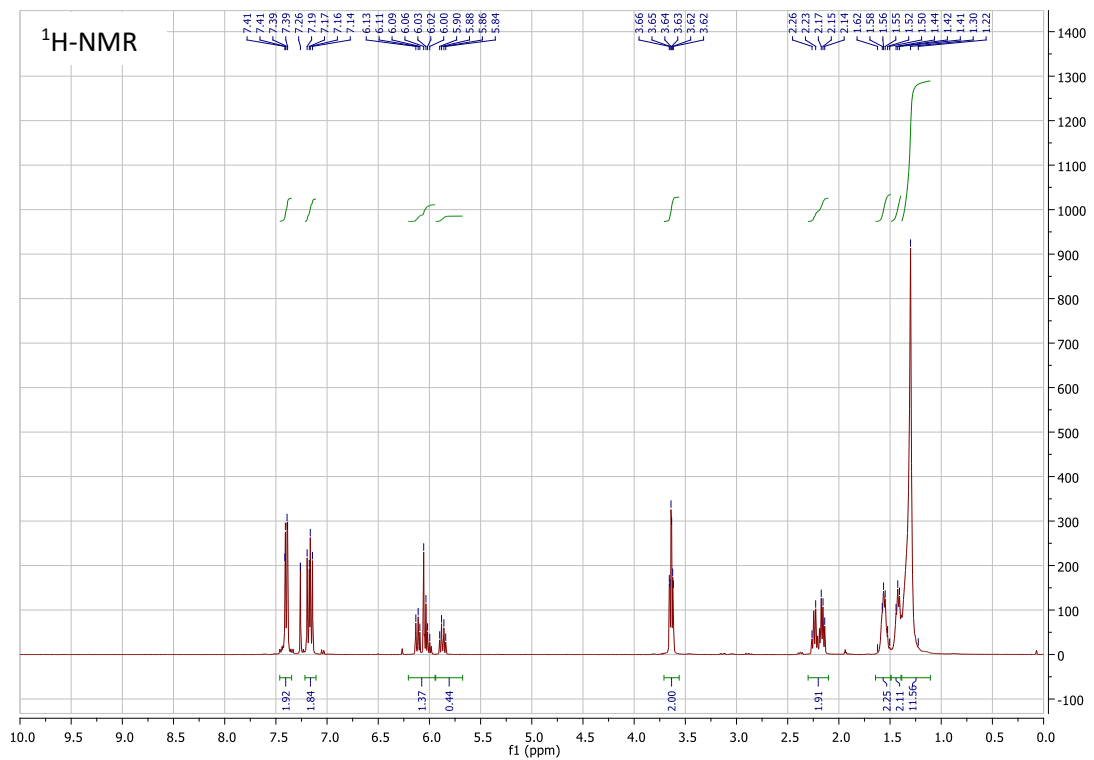
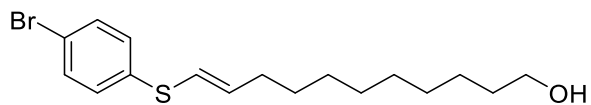


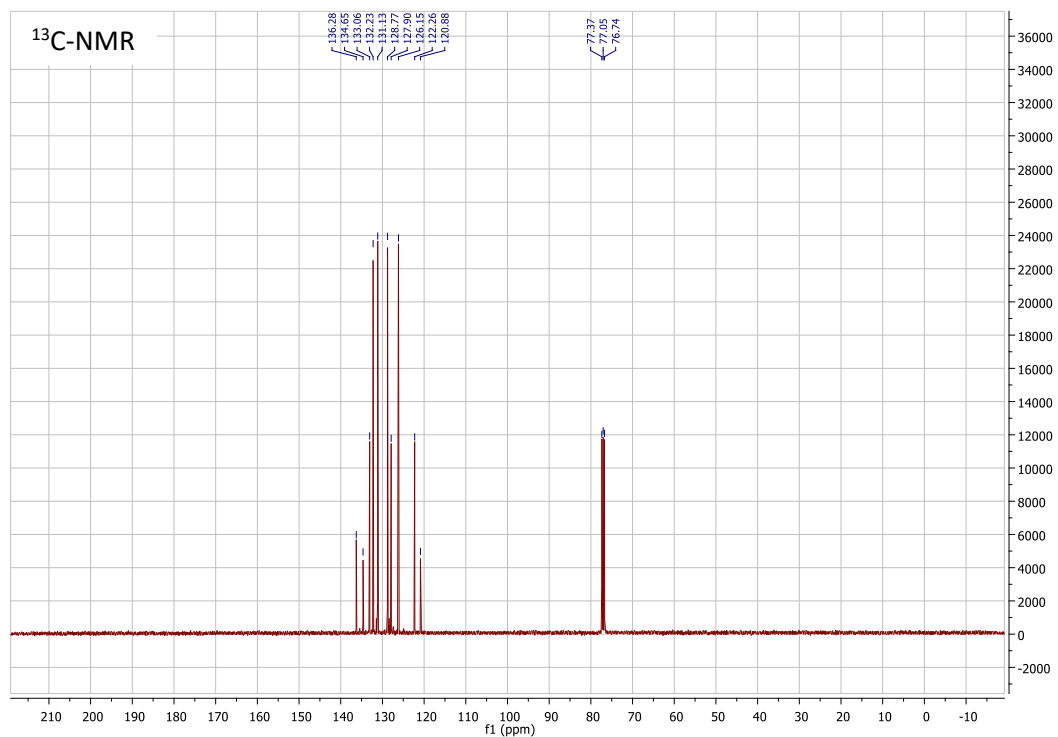
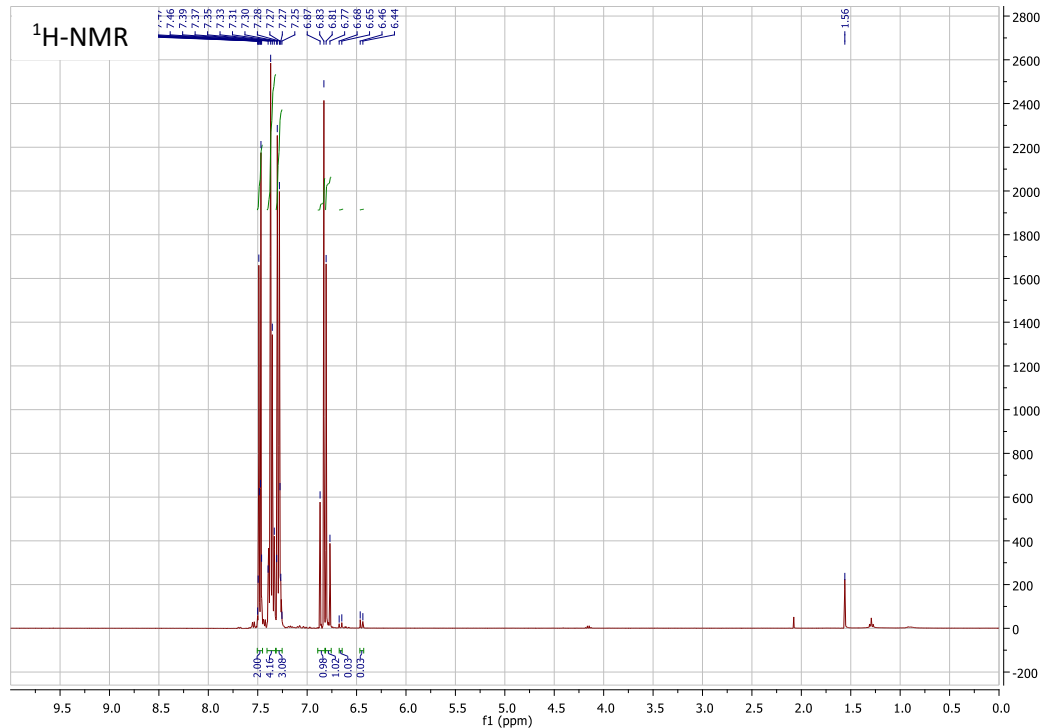
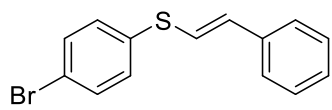


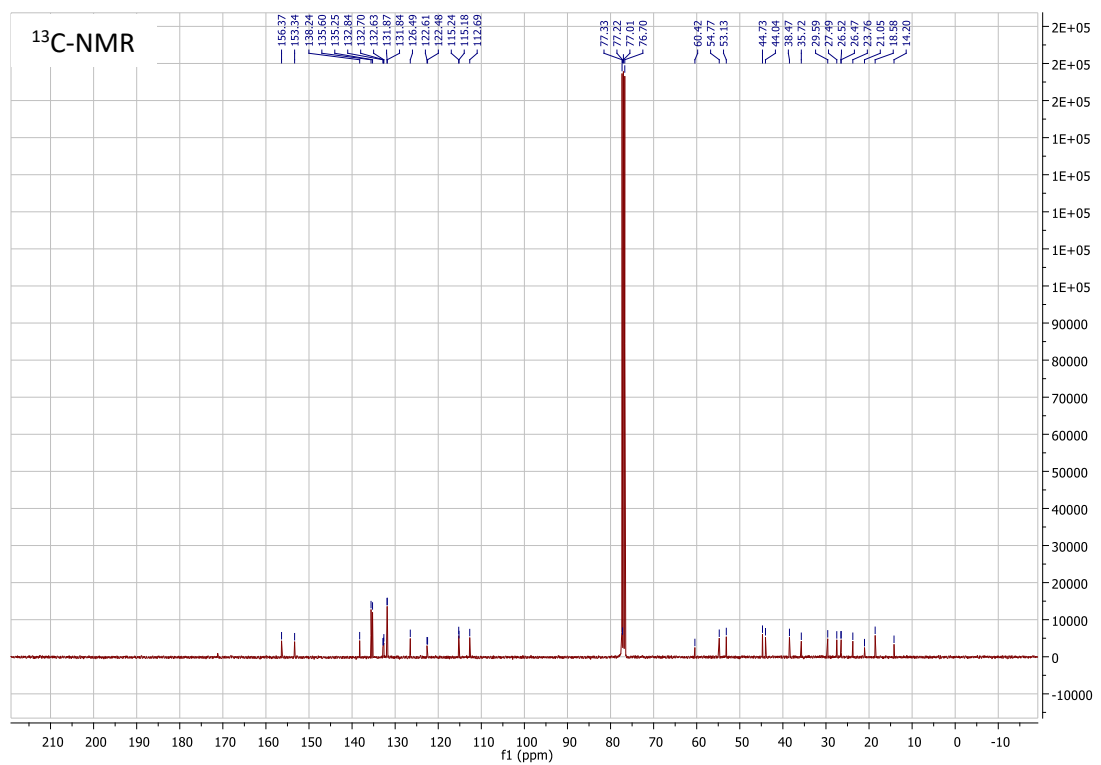
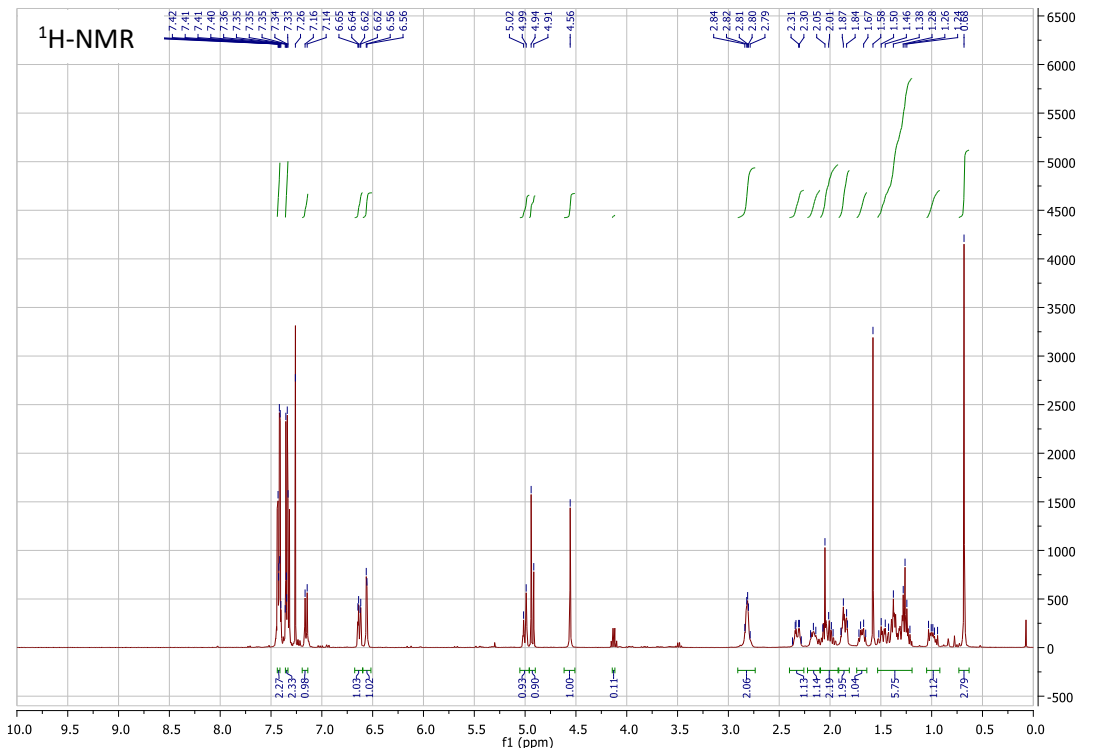
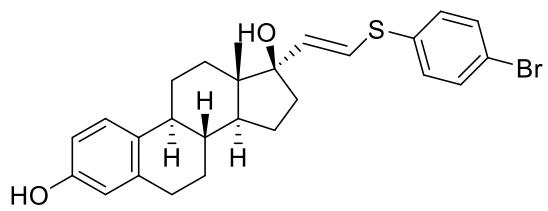


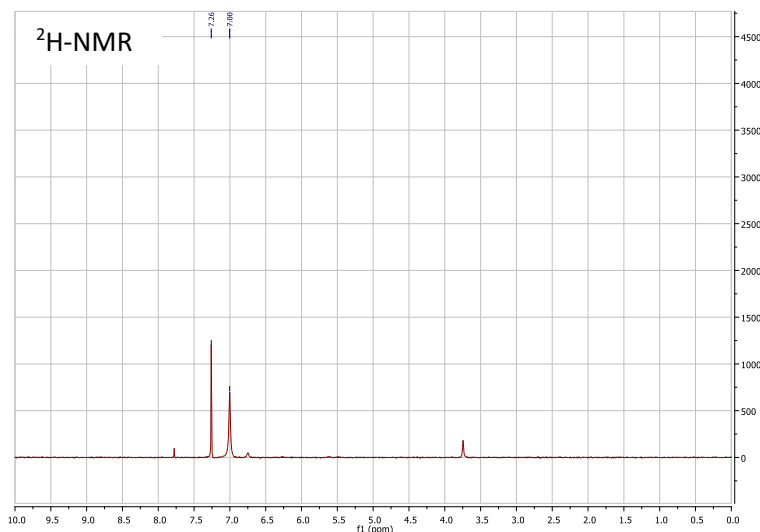
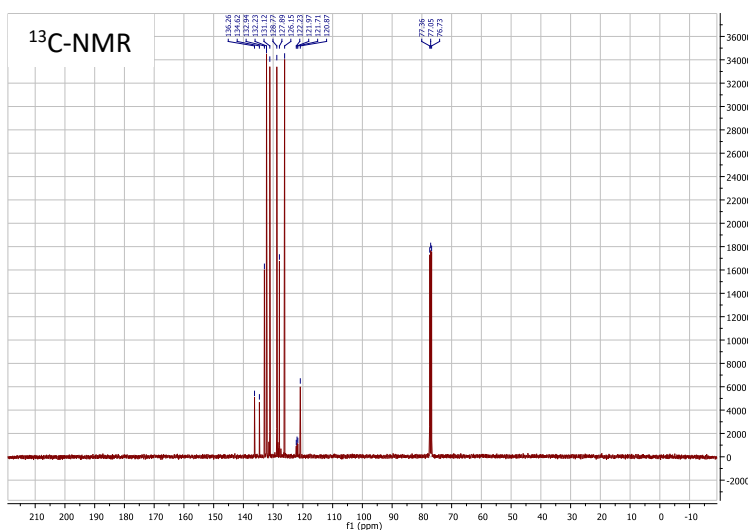
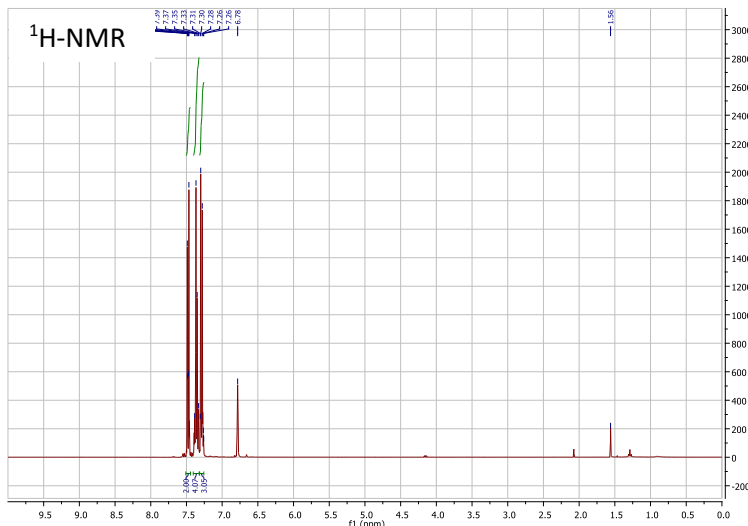
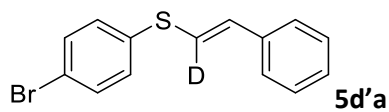


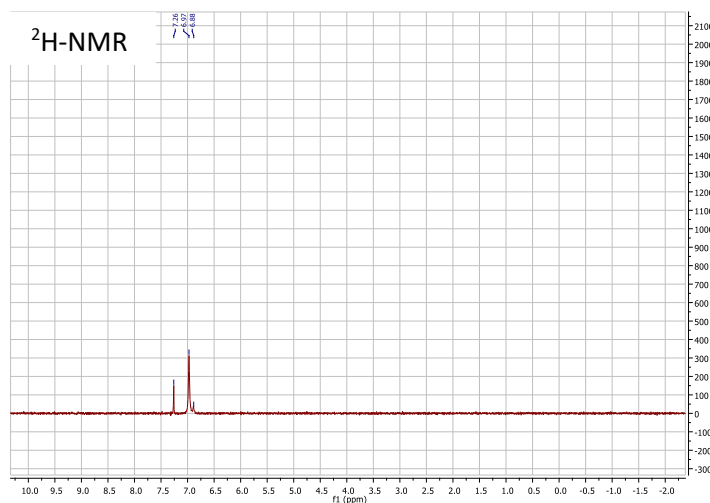
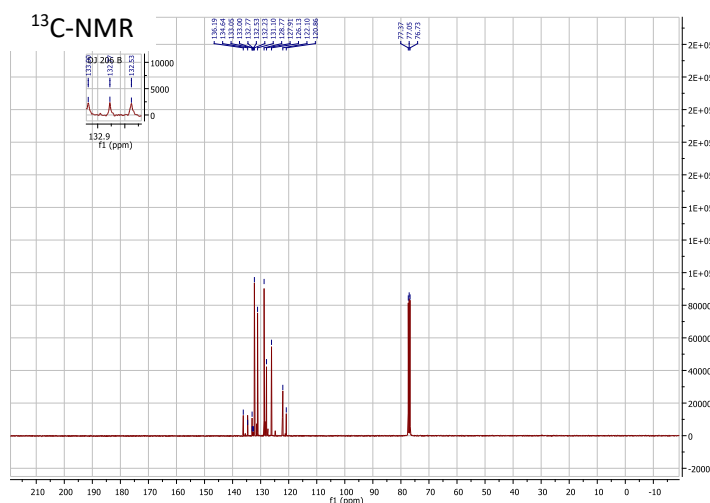
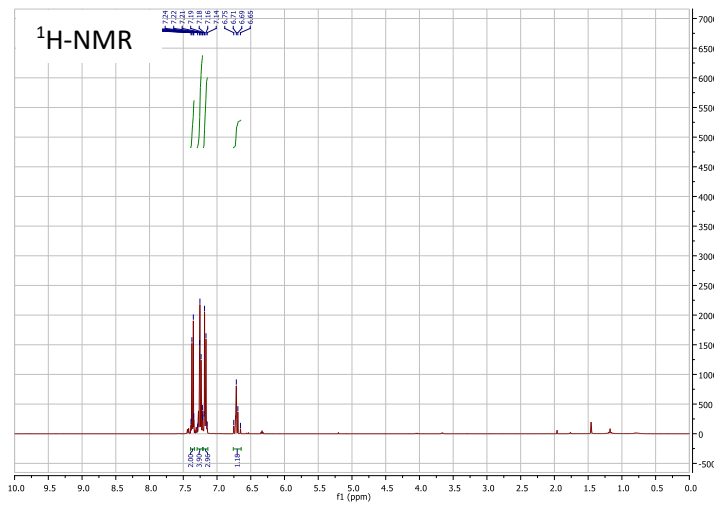
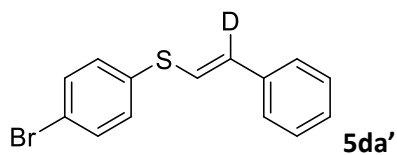












## 6. Supplementary Figures

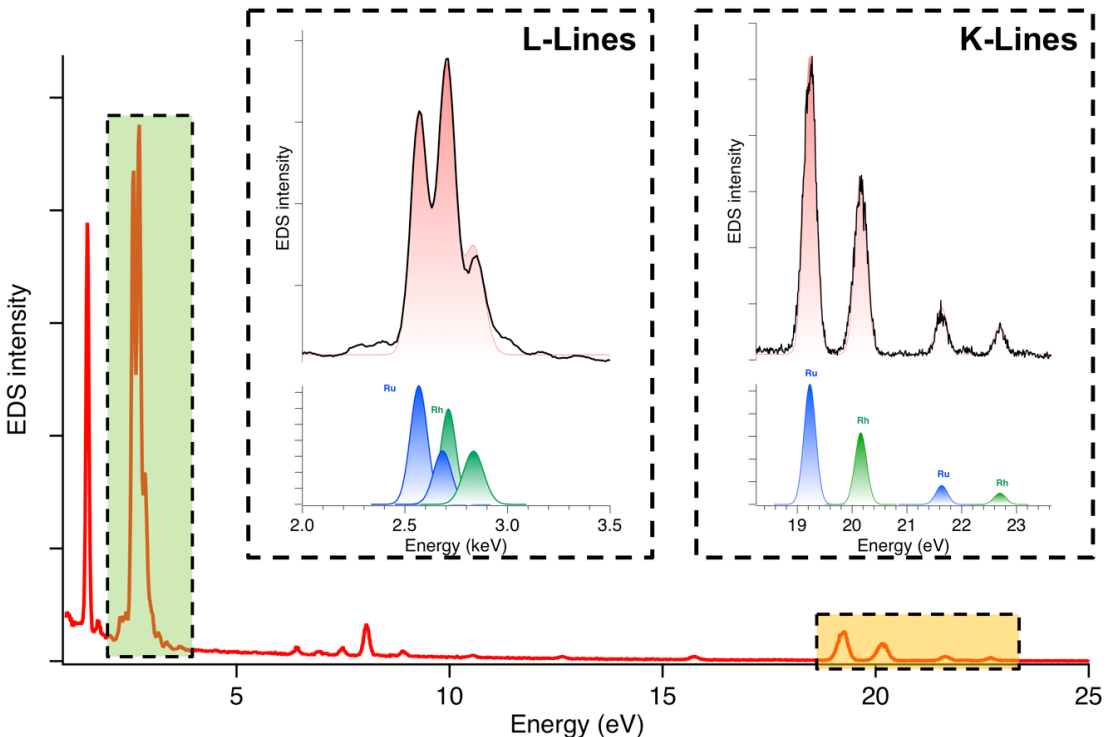


**Figure S1.** EDS spectrum integrated over the whole Figure 2b). Ru and Rh K-lines (orange box) and L-lines (green box) are zoomed in the insets. L-lines of both elements overlap whereas K lines are well-separated.

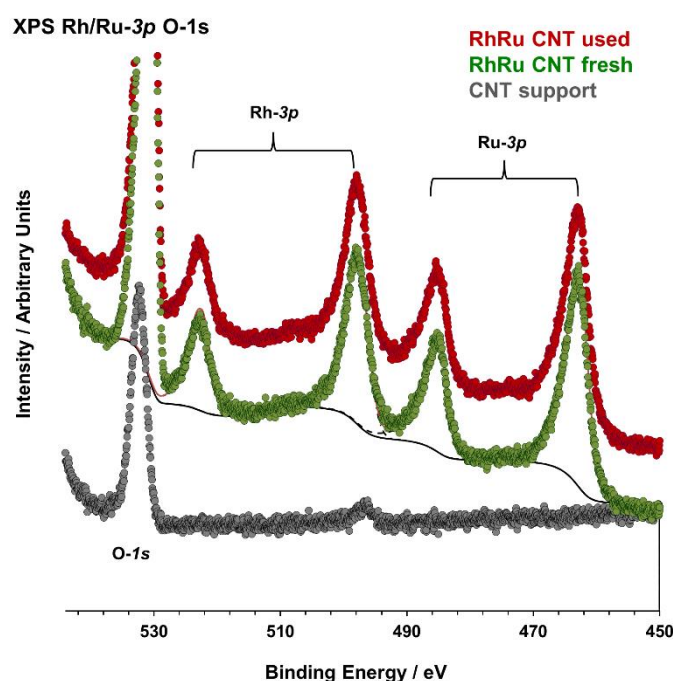


**Figure S2.** XPS spectrum showing Rh-3p, Ru-3p and O-1s regions for the nanotube support without metals (grey dots), the as-prepared hybrid catalyst (green dots), and the used catalyst (red dots).

### XPS Ru-3d C-1s

RhRu CNT used

RhRu CNT fresh

CNT support

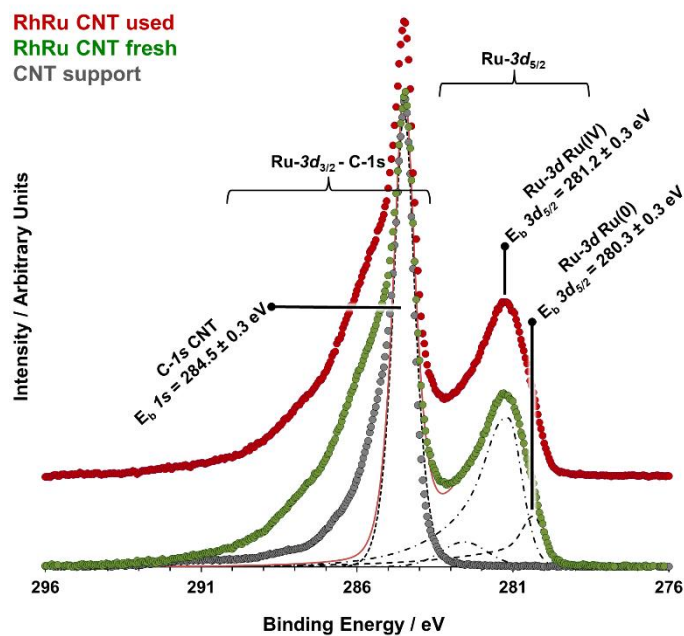


**Figure S3.** XPS spectrum highlighting the Ru(0) and Ru(IV) contributions (Ru-3d region) for the nanotube support without metals (grey dots), the as-prepared hybrid catalyst (green dots), and the used catalyst (red dots).

### XPS Rh-3d

RhRu CNT used

RhRu CNT fresh

CNT support

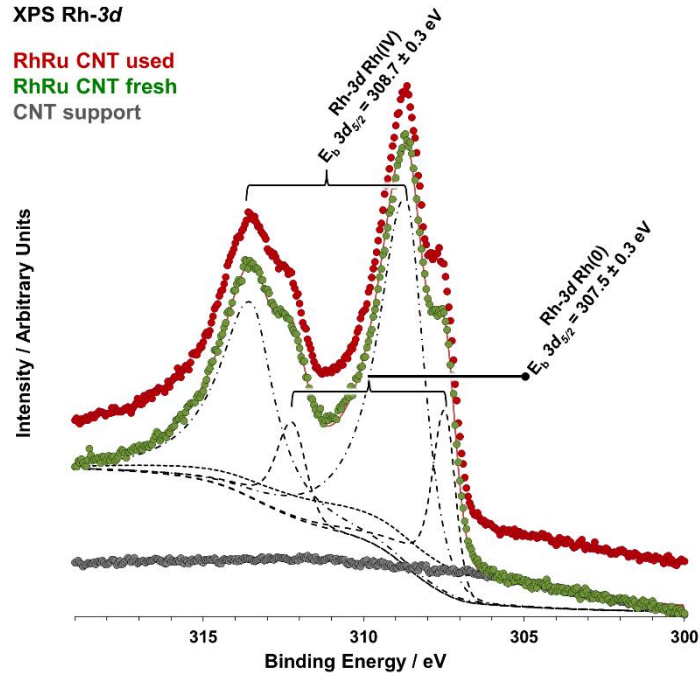


**Figure S4.** XPS spectrum highlighting the Rh(0) and Rh(IV) contributions (Rh-3d region) for the nanotube support without metals (grey dots), the as-prepared hybrid catalyst (green dots), and the used catalyst (red dots).

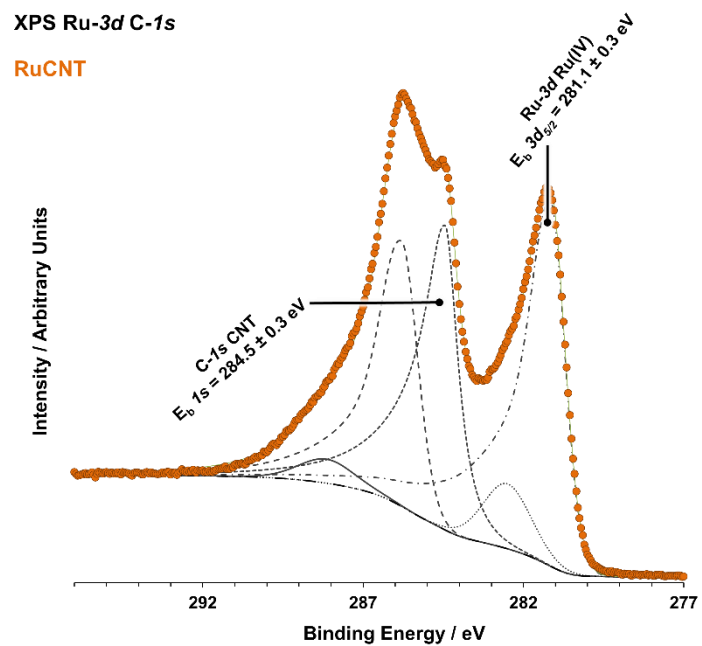


**Figure S5.** XPS spectrum showing the Ru-3d region of the monometallic RuCNT hybrid.

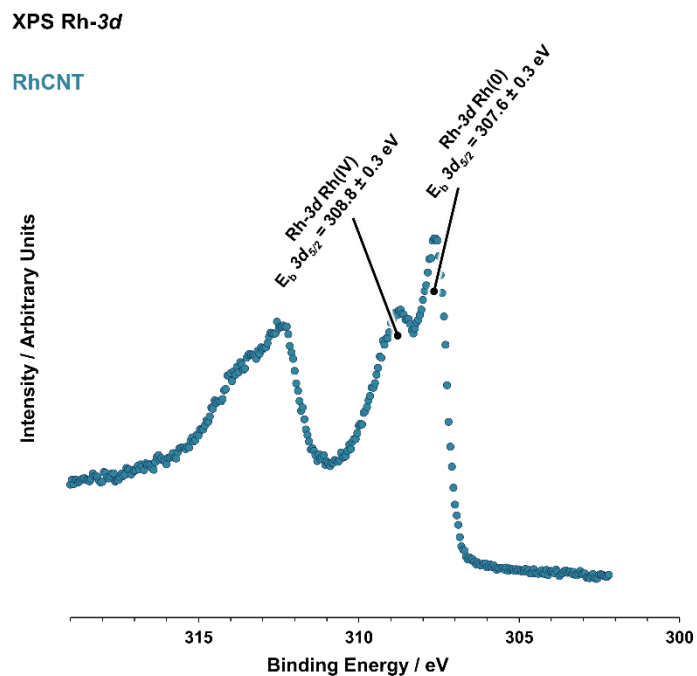


**Figure S6.** XPS spectrum showing the Rh-3d region of the monometallic RhCNT hybrid.

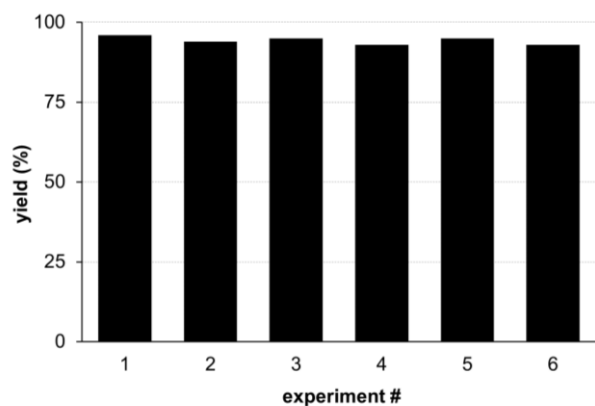


**Figure S7.** Recycling experiments.

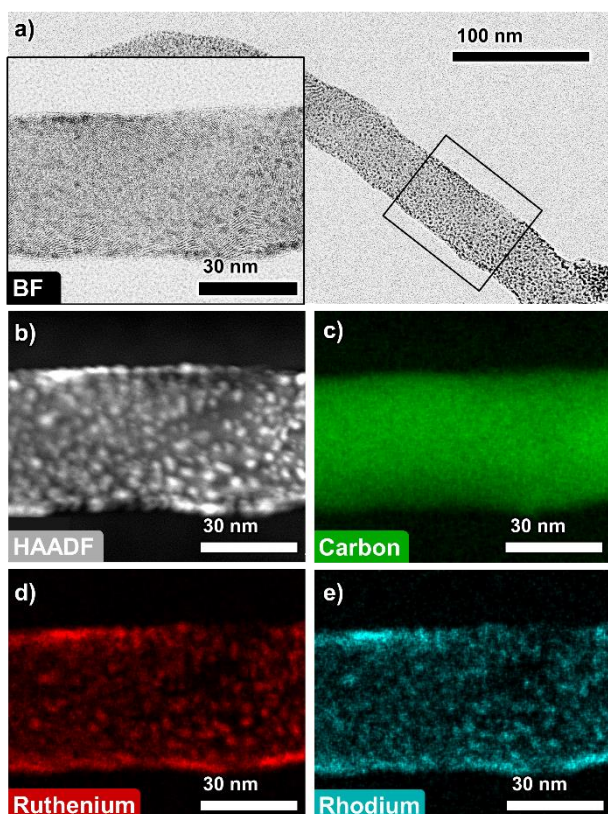


**Figure S8.** a) Bright field (BF) TEM image of the RuRhCNT hybrid recovered after catalysis, with higher magnification inset of the boxed area; b) High angle annular dark field (HAADF) image of the boxed region and associated EDS mapping for c) carbon; d) ruthenium; e) rhodium.

## 7. Supplementary Tables

**Table S1.** Comparison of the RuRhCNT system with representative state-of-the-art methodologies.

	Solvent	Additives	Temp. (°C)	Cat. / mol%	Recycling	Reference
<b>Heterogeneous systems</b>	RuRhCNT	EtOH	none	25	RuRh / 0.04	6 cycles (stable) This work
	Cu-NHC	DCE	N <sub>2</sub> atm.	70–100	Cu / 0.5	6 cycles (~15%) <i>Green Chem.</i> , 2014, <b>16</b> , 3916
	Rh-P-SBA-15	DCE	N <sub>2</sub> atm.	25	Rh / 1	4 cycles (stable) <i>J. Catal.</i> , 2018, <b>365</b> , 43
	Pd(hfpd) <sub>2</sub>	toluene	γ-terpinene (1 equiv.)	140	Pd / 0.01–0.1	no <i>Catal. Sci. Technol.</i> , 2018, <b>8</b> , 3073
	g-C <sub>3</sub> N <sub>4</sub>	MeCN	Xe lamp	25	Graphene / na	5 cycles (~10%) <i>Nanoscale</i> , 2021, <b>13</b> , 3493
	ZnIn <sub>2</sub> S <sub>4</sub>	MeOH	N <sub>2</sub> atm., LED light	25	Zn / 23, In / 46	3 cycles (stable) <i>Green Chem.</i> , 2019, <b>21</b> , 2345
	PDMVTI	DMF	none	60	Dimethylvinyl-thiazolium / 1	4 cycles (stable) <i>ChemCatChem</i> , 2016, <b>8</b> , 2476
	MCM-41-2P-RhCl(PPh <sub>3</sub> )	EtOH	none	40	Rh / 3	10 cycles (stable) <i>Catal. Lett.</i> , 2012, <b>142</b> , 138
<b>Homogeneous systems</b>	Tp*Rh(PPh <sub>3</sub> ) <sub>2</sub>	DCE/toluene	none	25	Rh / 3	no <i>J. Am. Chem. Soc.</i> , 2005, <b>127</b> , 17614
	[Pd] cat., L	DCM or toluene	Ar atm., TfOH or MsOH	40–60	Pd / 2–6	no <i>Org. Lett.</i> , 2019, <b>21</b> , 2213
	PPh <sub>3</sub> AuNTf <sub>2</sub>	THF	N <sub>2</sub> atm.	45	Au / 2	no <i>Org Lett.</i> , 2016, <b>18</b> , 2114
	Cp*ZrBn <sub>3</sub>	benzene	Ar Atm.	120	Zr / 5	no <i>J. Am. Chem. Soc.</i> , 2010, <b>132</b> , 10533
	Nil <sub>2</sub>	THF/MeCN	Li <sub>3</sub> PO <sub>4</sub> and HBpin	60	Ni / 10	no <i>Nat. Commun.</i> , 2019, <b>10</b> , 1752.
	[Rh(cod) <sub>2</sub> ]SbF <sub>6</sub>	DCE	N <sub>2</sub> atm. BINAP ligand	30	Rh / 0.1–1	no <i>J. Am. Chem. Soc.</i> , 2018, <b>140</b> , 10443
	ZnI <sub>2</sub>	DCM	TsOH	25	Zn / 10	no <i>J. Org. Chem.</i> , 2020, <b>85</b> , 6528
	Air/Δ-induced	AcOEt or CHCl <sub>3</sub>	TFA	66–80	none	na <i>Chem. Eur. J.</i> , 2020, <b>26</b> , 15804
	LB-catalyzed	DCM, Cy, or AcOEt	Ar atm., blue light	25	Lewis base / 0.5	na <i>J. Org. Chem.</i> , 2019, <b>84</b> , 8337

**Table S2.** Compilation of XPS data from the different hybrids.

	Ru-3d (E <sub>b</sub> 3d <sub>5/2</sub> , eV)		Rh-3d (E <sub>b</sub> 3d <sub>5/2</sub> , eV)	
	Ru(IV)	Ru(0)	Rh(IV)	Rh(0)
RuRhCNT	281.2	280.3	308.7	307.5
RuCNT	281.1	n.d.	/	/
RhCNT	/	/	308.8	307.6